MANDELA MINING PRECINCT
MINDS FOR MINES

TECHNICAL SERVICES OPTIMISATION

MMS22WP1: Developing an effective pillar design methodology for mechanised mining

Final Report

ENTERPRISES
University of Pretoria

Research agency: Enterprises University of Pretoria

Date: 13 March 2023

TABLE OF CONTENTS

1 EXECUTIVE SUMMARY

The objective of this study was to determine the most appropriate type of pillar strength formula to use when designing bord and pillar layouts. The type of formula needs to be clarified before it can be calibrated for different areas. It is not clear whether a linear formula may be better suited to describe the pillar strength in the South African mines compared to a power-law formula. This report describes the historic motivations for the different types of pillar strength formulae. The power-law strength formulae, made famous by Salamon and Munro (1967), were inspired by laboratory and underground experiments in the 1940s and 1950s. These original studies indicated that the strengths of square pillars of the same height vary as the square root of their widths. The strengths of pillars of the same width also vary in inverse ratio to their height. This was generalised by Salamon in a power-law formula with the familiar exponents with α and β. These exponents were subsequently calibrated using a database of failed and intact pillars. For the hard rock strength formula, Hedley and Grant (1972) used the same references of the 1940s and 1950s, as well as Salamon's work, to motivate the use of a power-law equation. In contrast, Bieniawski (1968) also did extensive underground experiments on different size coal specimens. An important finding of his study was that there is no change in strength once the specimen size exceeds 1.5 m. Based on this, he proposed the simpler linear pillar strength formula. Martin and Maybee (2000) list the important hard rock pillar formulae that were developed in later years based on observed pillar failures. Of significance is that all these take the form of either a power- or linear-type equation. As an important conclusion, owing to the large variability in datasets, there is not compelling evidence to use either a power-law or a linear pillar strength equation.

A literature study of the effect of cube specimen size on the compressive strength of rock in the laboratory was also conducted. This is important data as it may possibly give insight into the type of pillar strength formula that is applicable to South African hard rock pillars. All the studies reviewed indicated that laboratory rock strength decreases with increasing specimen size. This behaviour can be best described with a power-law, which includes the cube length as the controlling parameter. The exponent of this law has the typical value of ≈ -½. The drawback of this model is that it predicts that the pillar strength will eventually completely vanish for very large cube sizes. This is considered unreasonable and the model is probably only relevant to small laboratory-sized specimens. Bieniawski (1968) attempted to circumvent this problem by describing the strength after a critical size with a linear strength function. Some limited laboratory data of cube specimen testing for Merensky Reef is available, but further laboratory testing on Merensky Reef, UG2 and other chrome reefs is recommended to verify that a similar power-law applies to all the hard rock reefs studied in this project. An analysis of the available information is presented in the report to indicate that the exponent of the height parameter in the power-law pillar formula may require further study. Laboratory testing of rectangular prisms, with similar square bases but different heights, needs to be conducted to supplement the testing of cube specimens.

As a further step in the methodology of the project, a numerical and analytical modelling study was conducted to provide insight into which type of empirical strength equation can best describe the behaviour of the pillars at different width-to-height ratios. Previous researchers obtained results with a modified Hoek and Brown failure envelope with "brittle parameters" that predicted pillar strength curves that were in reasonable agreement with the observed empirical failure envelopes. These modelled curves are "upward increasing

concave" in contrast to another study where the modelled curve was "downward increasing concave". The well-known empirical power-law pillar strength equations (e.g. Salamon's coal pillar equation) are also increasing concave downwards in shape and it can therefore not simulate the transition to squat pillar behaviour at large width to height ratios. It is apparent that the major differences between many empirical pillar strength relationships are characterised by the evolution of the pillar strength curvature, represented by the sign of the second derivative as a function of the pillar width to height ratio. An analytical limit equilibrium model, similar to the failure model used in the TEXAN code, was studied for this project. It predicted pillar strength as a function of the width to height ratio that is upward concave, similar to the Hoek and Brown models. The limit equilibrium model, with a spalling transition region, can replicate the behaviour of empirical formulas for pillar strength, including the transition to so-called "squat" pillar behaviour. This seems to be an attractive model to simulate the observed pillar strength as a function of width-to-height ratio. As a further contradiction, however, the modelling conducted for this report of a single pillar using the FLAC3D code indicated that the strength curve has an increasing concave down shape.

From these various studies, it is concluded that significant uncertainty still exists in terms of the best equation to describe the pillar strength behaviour and this can only be resolved using further laboratory testing and underground observations of pillar behaviour. Both the power-law and linear formulae, and variations of these, are widely used. It appears that the problem of finding a "universal" strength equation is caused by the variability in the measured strength of pillars, both in the laboratory and in actual mines. It is difficult to fit strength equations to the results because of the wide scatter of the data. This is a significant finding that can be used to guide future research. The report also describes another four key areas where there is a gap in knowledge. These are the effects of loading stiffness on pillar stability, naturally occurring variability in pillar strength, the best method to do reclamation of hard rock pillars in mature mines and the effect of shear stress on pillar strength. Based on these many considerations, a different approach in terms of future research is proposed. To make a meaningful contribution in a short period of time, it is proposed that future work focus on two aspects. These are back analyses of carefully selected bord and pillar layouts to estimate pillar strength and numerical modelling of the loading system stiffness.

2 AIM OF RESEARCH PROGRAMME

This work is an extension of the project MMS21WP1 Rock Engineering Pillar Design. The first project was used to scope a possible future project to determine an effective pillar design methodology for mechanised mining operations. A key aspect to clarify before commencing with the proposed expensive laboratory and underground experimental work is to determine the most appropriate type of pillar strength formula to use. The type of formula needs to be decided upon before it can be calibrated for different areas. A key hypothesis tested in this project was whether a linear formula may be better suited to describe the pillar strength in the South African mines compared to a power-law formula. A final objective of this project was to scope future research to make meaningful progress in terms of quantifying pillar strength.

3 METHODOLOGY USED

The methodology of the project consisted of a number of components. These included a comprehensive literature survey of the types of formulae used to design pillars and a literature study of laboratory experiments on various specimen sizes and numerical modelling. Additional numerical modelling and an analytical pillar strength solution were also used to study this problem. The information collected was collated and analysed to determine if an appropriate type of pillar strength formula for South African conditions could be identified.

4 RESEARCH FINDINGS

The following sections give an overview of the important results obtained during this project.

4.1 Origins of the pillar strength formulae

4.1.1 Early motivation for the adoption of a power-law pillar strength formula for coal

The Coalbrook disaster was a major stimulus for rock engineering research and specifically the study of coal pillar strength. The research program was directed by the Coal Mining Research Controlling Council and the work was conducted by the Collieries Research Laboratory of the Chamber of Mines of South Africa. As part of this research, Salamon and Munro (1967) analysed 125 case histories, of which 27 were collapsed pillars. They proposed that the coal-pillar strength could be determined using the power-law formula:

$$\sigma_p = K\frac{w^\alpha}{h^\beta} \tag{1}$$

where σ_p (MPa) is the pillar strength, K (MPa) is the strength of a unit volume of coal, w is the width of the pillar and h is the mining height. The selection of a power-law is interesting and important and it was motivated in their paper as follows:

"*Attempts have been made by several workers to determine the strength of mineral pillars. Greenwald, Howarth and Hartmann (1939) in the United States tested coal specimens underground with maximum dimensions of up to five feet, and derived an empirical formula for pillar strength. Steart (1954) published a similar expression on the basis of laboratory testing of coal and reasoning. The same formula was proposed, as a result of fairly extensive laboratory tests, by Holland and Gaddy (1957) for coal pillars. More recently, Skinner (1959) arrived at a formula for predicting the effect of volume change on the strength of pillars using a statistical technique (the weakest link theory) to extrapolate the results of small-scale tests on anhydrite. The strength of a pillar depends on the strength of the material of which it is composed, its volume and its shape. Presumably, the effect of shape is due to the constraint imposed on the pillar by the roof and floor through friction or cohesion. The volume and shape* *of square pillars are completely defined by their width (w) and height (h). The most commonly-occurring pillar strength formula in the literature is a simple power function composed of these variables*."

The last sentence in the quote is of particular importance. Equation (1) was therefore adopted by Salamon and Munro (1967) as it was "*the most commonly-occurring pillar strength formula in literature*". This was explored in more detail for this project by studying the papers referred to in this quote.

The Greenwald et al (1939) paper could not be found, but Greenwald et al (1941) give the necessary insight into their equation as it was an extension of the work published in 1939. Coal pillar experiments were conducted by the authors. Small pillars were formed underground and a slot was cut at the top of the pillar to install a loading device. Pillars with different w:h ratios were tested. Based on these test results, they derived the following equation for the strength, S, of the pillars:

$$S = 2800\frac{\sqrt{w}}{\sqrt[6]{h^5}}\ (\text{lb/in}^2) \tag{2}$$

This can be written as

$$S = 2800\frac{w^{\frac{1}{2}}}{h^{\frac{5}{6}}} \tag{3}$$

This is therefore similar to equation (1) with $\alpha = \frac{1}{2}$ and $\beta = \frac{5}{6}$.

The paper by Steart (1954) was also sourced. From laboratory experiments on coal specimens, he noted that three rules apply:

Rule 1 - The strengths of pillars of the same width vary in inverse ratio to their height (Figure 1).

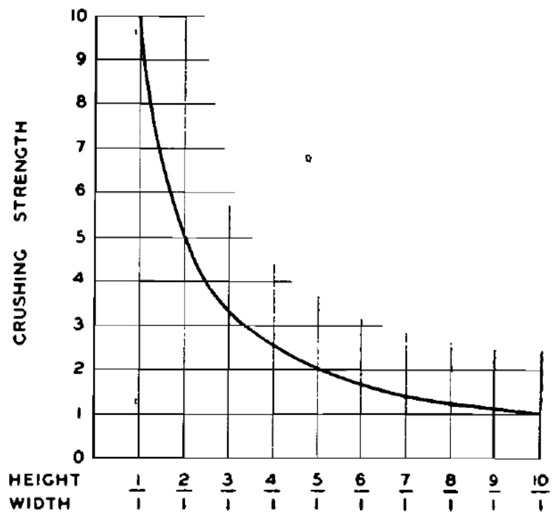

Figure 1. Steart's Rule 1 for coal pillars.

Rule 2 - The strengths or resistance to crush, of square pillars of the same height, varies as the square root of their widths (Figure 2).

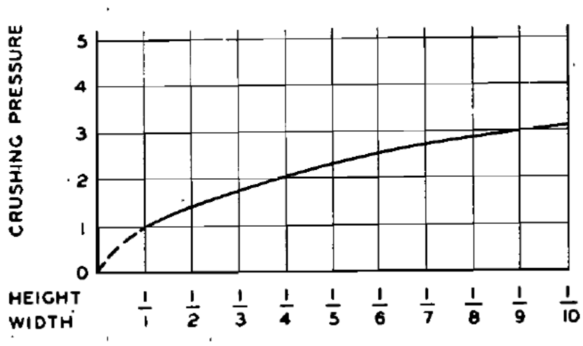

Figure 2. Steart's Rule 2 for coal pillars.

Rule 3 - The strengths of pillars of cube form vary in inverse ratio of the square root of their dimensions (Figure 3).

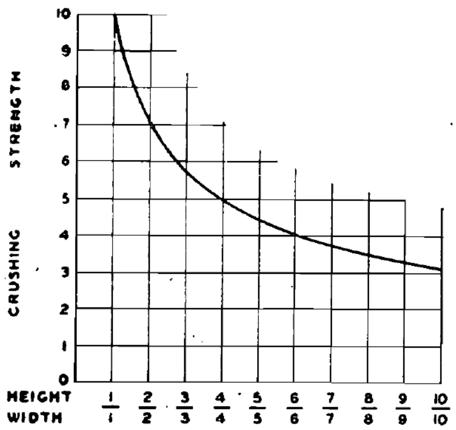

Figure 3. Steart's Rule 3 for coal pillars.

Based on these observations, Steart (1954) calculated the coal pillar strength for a number of practical case studies. He did not give a general symbolic pillar strength formula in the paper, but strength calculations using actual values are presented. For example, if the crushing strength of a 1 ft cube of coal is 140 tons, then the crushing strength of a 100 ft wide square pillar with a height of 4 ft is:

$$Crushing\ strength = 140\frac{\sqrt{100}}{4}\ \text{(tons per sq. ft)} \tag{4}$$

This equation is therefore similar to the form of equation (1) with $\alpha = \frac{1}{2}$ and $\beta = 1$.

Furthermore, the notion that the strength of a rock mass is to a large part controlled by the geometry of the specimen, i.e., the width-to-height ratio, has since been confirmed by extensive laboratory studies (see Hudson et al, 1972).

After adopting the power-law formula in equation (1), Salamon and Munro (1967) conducted a statistical analysis on data from 125 case studies. This gave the following values for the parameters in equation (1): K = 7.176 MPa, $\alpha = 0.46$ and $\beta = 0.66$. This has been applied extensively to the design of pillar layouts in South Africa since its introduction in 1967. As this is an empirical equation, it must always be considered that it was originally developed for room and pillar mining of horizontal coal seams with square pillars and that the values of the parameters are only applicable to South African coal.

4.1.2 Early studies of the strength of hard rock pillars

An early investigation into the design of hard rock pillars was carried out by Hedley and Grant (1972). They studied 28 rib-pillars (3 crushed, 2 partially failed, and 23 stable) in massive quartzites and conglomerates in the Elliot Lake room and pillar uranium mines. They also used equation (1) as a basis for their strength formula and derived $K = 179\ MPa$, $\alpha = 0.5$ and $\beta = 0.75$. The parameter K was determined from extrapolation of laboratory tests and it was estimated that its value is "*26 000 psi for a 1-ft cube*". K was later reduced to 133 MPa (Hedley at al, 1984). The reason for adopting equation (1) is given in their paper as: "*The relationship between pillar dimensions and strength is usually expressed in the form* (of equation (1))" The references they gave for this was Salamon and Munro (1967), Greenwald et al (1939), Steart (1954) and Holland and Gaddy (1957). They therefore used exactly the same motivation as Salamon and Munro (1967) for adopting a power-law strength formulation for hard rock, although the early work they referred to was done on coal.

The uranium mines in the Elliot Lake area used a stope-and–pillar layout to mine the orebody. Narrow pillars of about 250 ft (76 m) were left along dip (see Figure 4). The pillars on which the analyses were conducted were typically 10 - 20 ft wide (≈ 3 – 6 m) and 8 – 20 ft high (≈ 2.5 – 6 m). The width to height ratio of most of the pillars was close to 1 and only a very few (3 in the database) had a width to height ratio of 2.5. It is clear that this original formulation was derived for slender rib pillars and it can be questioned whether it is applicable to square pillars with a width to height ratio greater than 2.5. The original data used by Hedley and Grant is reproduced in Figure 5. It is immediately obvious that the dataset used was very small (28 pillars). The width to height ratio of the failed pillars varied from 1.1 to 1.5. Only 3 of these pillars were "crushed" and 2 were "partially crushed". Of further concern is that it is stated in the paper that: "*The information on complete pillar crushing was obtained second-hand because it happened in mines which are closed*." This work was conducted in the days before computer-based numerical modelling could be used to determine pillar stress. The approach followed was to use tributary area theory. The stress given in the table in Figure 5 for each pillar is therefore only a rough estimate. They also acknowledge that this equation refers to square pillars, whereas those in the uranium mines are long and narrow. Their assumption was that the strength of the slender pillars would not be much greater than that of a square pillar of width equalling the minimum width of the long pillar.

Appropriate values for parameters α and β had to be derived by Hedley and Grant (1972). Three different sets of values for the failed pillars were available to them. The value for α was relatively constant at 0.5 and they therefore decided to also adopt this value. As β varied more, a new value was computed and their approach was to focus on the three failed pillars in the database. For each of these pillars, the tributary area stress in the table (Figure 5) was assumed to be the pillar strength. This value, as well as the K-value and $\alpha = 0.5$ were inserted into equation (1). For each pillar, the value of β was solved. The three values ranged from 0.736 to 0.768 with an average of 0.75. This value was adopted and it resulted in the now familiar Hedley and Grant formulation.

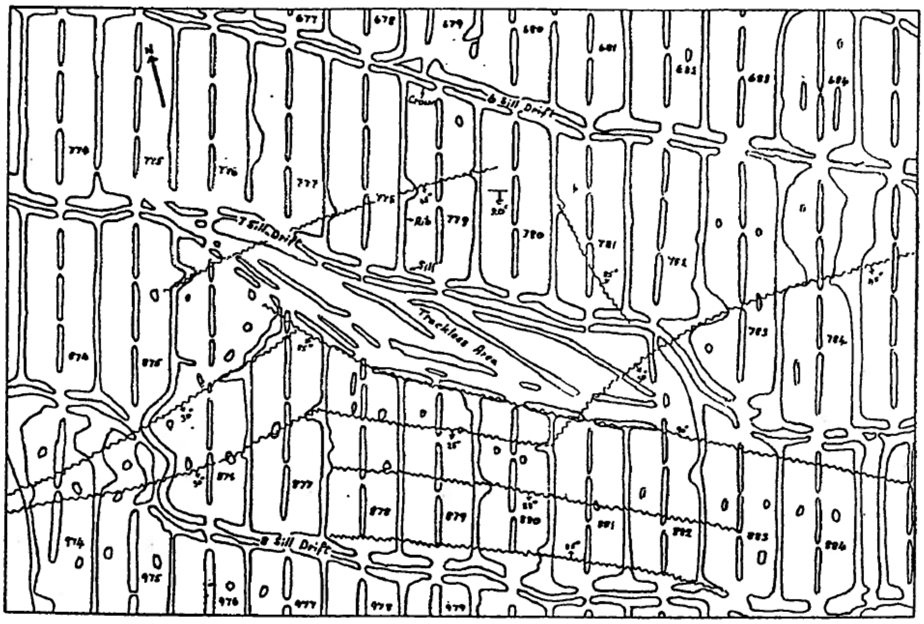

Figure 4. Typical layout of a mine in the Elliot Lake district (after Hedley, Roxburgh and Muppalaneni, 1983).

TABLE 3 — Dimensions and Estimated Stress and Strength of Pillars

Depth ft	Dip deg.	Extraction %	Pillar Width ft	Pillar Height ft	Estimated Pillar Stress psi	Estimated Pillar Strength psi
Stable Pillars						
500	17	85	10	10	5000	14600
700	17	85	10	10	6400	14600
800	26	65	20	18	3800	13300
850	20	85	10	10	7600	14600
950	11	85	10	10	7500	14600
1000	22	65	20	18	4000	13300
1050	15	85	10	10	8500	14600
1200	18	85	10	10	9400	14600
1300	20	65	20	20	4600	12300
1600	20	60	20	18	4800	13300
1600	20	65	18	18	5400	12600
1600	22	75	20	14	7600	16000
1700	22	65	40	20	5800	17400
1700	22	60	22	20	5000	12900
1700	12	75	20	14	7600	16000
1800	5	75	20	14	8000	16000
1900	23	65	19	18	6400	13000
2200	25	65	20	20	7200	12300
2400	11	65	20	8	7600	24400
2500	9	65	20	8	7900	24400
2700	13	65	20	8	8600	24400
2900	12	70	15	9	10500	19400
2900	12	75	20	9	12600	22400
Partially Failed Pillars						
1400	20	85	10	10	11400	14600
2400	18	80	10	9	13400	15800
Crushed Pillars						
2800	12	80	10	9	15200	15800
2900	12	80	10	9	15700	15800
3400	5	80	15	10	18500	17900

Figure 5. A reproduction of the original dataset used by Hedley and Grant (1972) to calibrate their power law formulation for hard rock pillar strength.

Regarding South Africa, based on the success of the Salamon and Munro strength formula in the coal mines, it was natural for the shallow hard rock mines to adopt a similar power-law strength formula. The necessary research was, unfortunately, never conducted to develop and calibrate a formula for local conditions. Instead, the Hedley and Grant (1972) formula was adopted. Only the K-value was modified to reflect local rock strengths. This approach seemed to work well and over the years it has become firmly entrenched. Ryder and Jager (2002) comment that this original formulation: "*for want of local data, have subsequently been applied in South African hard-rock mines*". The first use of this formula in a South African mine is not clear, but Ozbay et al (1995) stated that it was "popularized by Wagner and Salamon (1979) as quoted by Kersten (1984)". Kersten used it to design pillars for Agnes Gold Mine. Subsequently, it was used to design a large number of bord and pillar layouts with an adjusted value for K. The rule frequently used in South Africa is to estimate K at between one-third and two-thirds of the UCS of the pillar material (e.g. see Ozbay et al. 1995). Almost no collapses in the Bushveld have been reported to date using this formulation, except where weak clay layers are present in the pillar (see Couto and Malan, 2023).

4.1.3 The alternative "linear" formula

Bieniawski (1968) tested cubical coal specimens measuring from 0.75 in. - 6.6 ft (2 cm to 2 m) in size. An important finding of his investigation was that:

"*there appears to be no more change in strength once the specimen size of 5 ft (1.5 m) is reached. Consequently, from this size onwards the strength of specimens will be the same in spite of their increasing dimensions. Thus, a 20 ft cube coal pillar would have the same strength as a 5-ft cube coal specimen which means that results of such in situ tests are directly applicable to the design of full-size coal pillars. It also means that the strength of coal mass is reached by relatively small finite size coal specimens and not specimens of infinitely large dimensions as predicted theoretically*."

Figure 6. Experimental setup for testing small coal specimens underground (after Bieniawski, 1968).

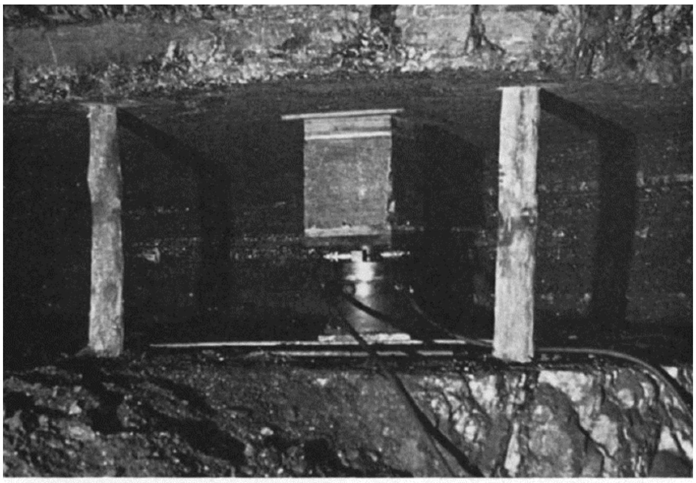

Figure 7. Loading arrangement for underground testing of medium-sized coal specimens (after Bieniawski, 1968).

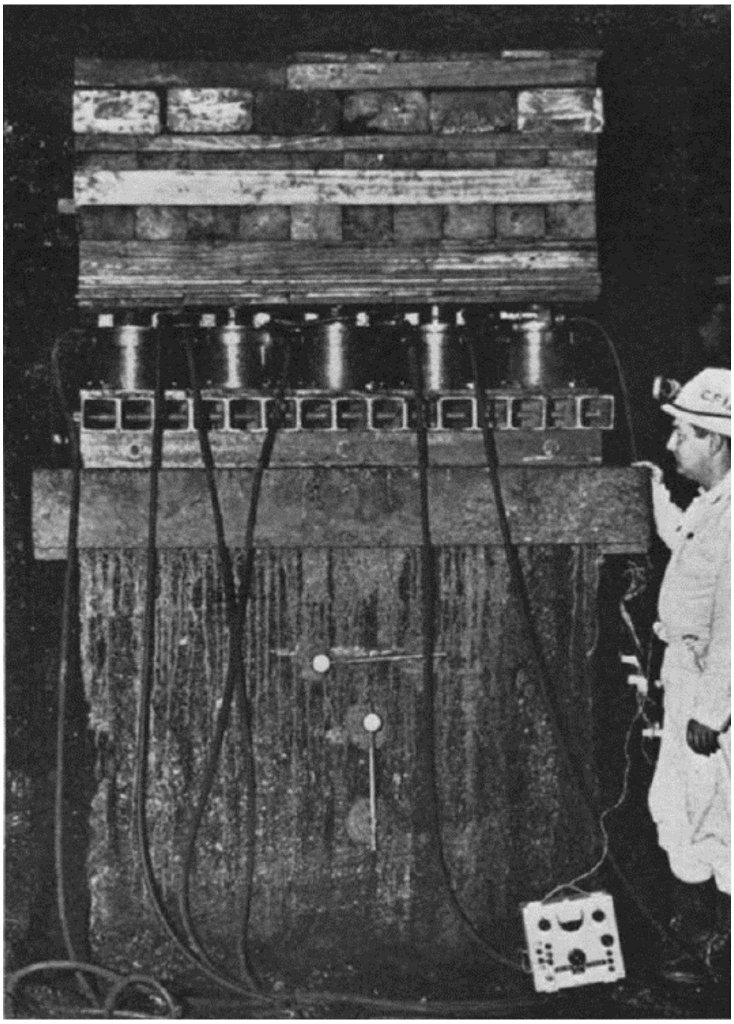

Figure 8. A large-size coal specimen with loading and monitoring system (after Bieniawski, 1968).

Based on this work, Bieniawski proposed a linear equation of the following form for coal specimens with $\frac{w}{h} > 1$ and specimen sizes larger than 5 feet (1.5 m):

$$\sigma_p = 400 + 220\frac{w}{h} \tag{5}$$

The units of equation (5) is (lb/in^2). A general form of the 'linear' equation, with no volumetric size effect, was proposed by Bieniawski and Van Heerden (1975) and Bieniawski (1992) and it directly expresses the strengthening effect of the w:h ratio:

$$\sigma_p = K\left(A + B\frac{w}{h}\right) \tag{6}$$

In this equation, K (MPa) is the "in-situ" strength of a large block (w:h = 1) of pillar material and A and B are dimensionless strengthening parameters and it is required that A+B = 1. Ryder and Jager (2002) state: "*The power law and its derivatives are perhaps too entrenched in coal engineering to warrant withdrawing from them at this time, but in hard rock engineering, the simpler and probably more realistic linear forms are advocated for general use*."

York and Canbulat (1998) compared the relative goodness-of-fit power formula versus linear forms for both coal and hard rock materials, and concluded the latter behaved at least as well. An objection raised by Bieniawski (1992) is that, according to the power-law formulation, the cube strength (w = h) would continue to decrease indefinitely with side length. This is considered unreasonable (Hustrulid, 1976). Most laboratory and field data indicate that the w:h strengthening curve has a zero or positively upwards curvature (Ryder and Jager, 2002). In contrast, the power law formula predicts downward curvature.

4.1.4 Additional formulae to predict hard rock pillar strength

Following the work by Hedley and Grant (1972) there have been several other attempts to develop hard-rock pillar strength formulae. These are given by Martin and Maybee (2000) and are listed in Table 1. It is clear the formulae take the form of either power- or linear-type equations, and that these equations have been used to predict the pillar strength for a wide range of pillar shapes and rock mass strengths.

Table 1. Different empirical strength formulae for hard rock pillars (after Martin and Maybee, 2000).

Reference	Pillar strength formulas (MPa)	σ_c (MPa)	Rock mass	No. of pillars
[3]	$133\frac{W^{0.5}}{H^{0.75}}$	230	Quartzites	28
[4]	$65\frac{W^{0.46}}{H^{0.66}}$	94	Metasediments	57
[5]	$35.4(0.778+0.222\frac{W}{H})$	100	Limestone	14
[6]	$0.42\sigma_c\frac{W}{H}$	—	Canadian Shield	23
[7]	$74(0.778+0.222\frac{W}{H})$	240	Limestone/Skarn	9
[8]	$0.44\sigma_c(0.68+0.52\kappa)$	—	Hard rocks	178[a]

The references referred to in Table 1 are: [3] Hedley and Grant (1972); [4] Von Kimmelmann (1984); [5] Krauland and Soder (1987); [6] Potvin et al (1989); [7] Sjöberg (1992); [8] Lunder and Pakalnis (1997).

The paper by Sjöberg (1992) was sourced and his equation is based on the data given in Figure 9. This was for sill pillars in the open stope mining layout at the Zinkgruvan mine in Sweden. This figure with its sparse data illustrates that care should be exercised with the published pillar formulae as it is typically based on very limited data and crude assumptions. For example, a power-law could have also been used for the data in Figure 9. No good reason is given for the adoption of a linear formula.

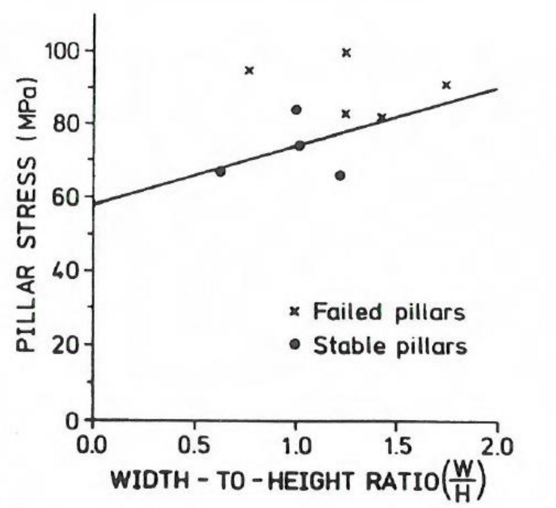

Figure 9. Calculated average pillars stress versus pillar w:h ratio (after Sjöberg, 1992).

Sjöberg (1992) fitted a line through the data in Figure 9. It is not clear how this line was fitted and he could have selected a slightly larger y-intercept and a smaller slope. His line yielded the equation:

$$\sigma_p = 58 + 16\frac{w}{h} \tag{7}$$

This can be re-written as:

$$\sigma_p = 74\left(0.78 + 0.22\frac{w}{h}\right) \tag{8}$$

A comparison of the pillar strengths predicted by the formulae given in Table 1 are illustrated in Figure 10.

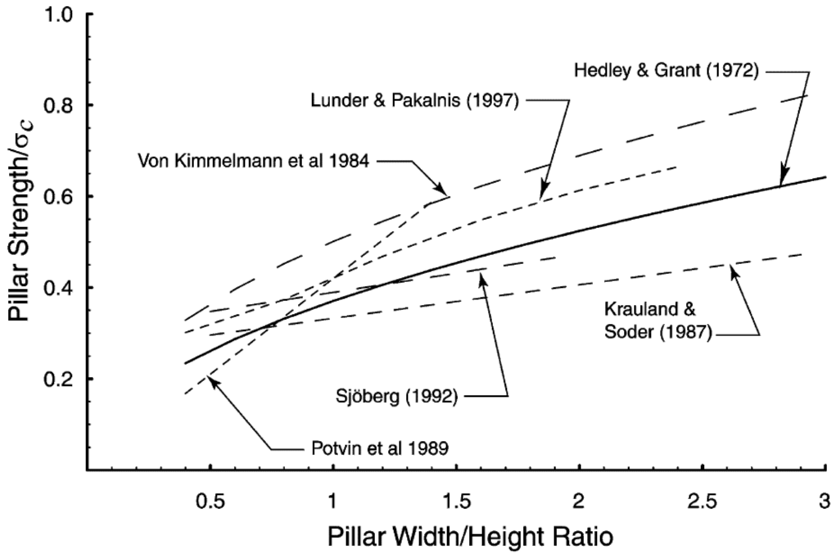

Figure 10. A comparison of the pillar strength formulae given in Table 1 by using a pillar height of 5 m (after Martin and Maybee, 2000).

From Figure 10, it is clear that these formulae predict approximately similar strengths, especially if the pillar w:h ratio is between 0.5 and 2.5. The pillar-strength formulas ignore the effect of σ_3, except the Lunder and Pakalnis (1997) formula, and rely on a simple stress to strength ratio based on the maximum pillar stress and the uniaxial compressive strength. While Lunder and Pakalnis (1997) attempt to include the effect of σ_3, by including the parameter κ , their formula predicts similar strengths to the other formulas.

4.1.5 The effect of the exponents on the behaviour of the power-law formula

The use of empirical power-law strength formulae is the standard method to determine pillar strength in the South African mining industry. Equation (1) matches the expected behaviour of a pillar, where an increase in the width and a decrease in the height of the pillar will result in an increase in strength. The more difficult part is the calibration of the constants K, α and β for a particular reef type.

As discussed above, the parameters α and β are equal to 0.46 and 0.66 respectively in the Salamon and Munro (1967) coal pillar strength formula. This was developed using a South African database of failed coal pillars and the formula served the coal industry well for several decades.

For the Hedley and Grant (1972) formula, α = 0.5 and β = 0.75. These exponents were also adopted for South African hard rock mines (all commodities) and it was never verified or questioned until limited PlatMine research was done in the 2000s (Watson et al., 2008). When using the Hedley and Grant formula, the estimation of the K-value is problematic and is typically assumed to be between a third and two thirds of the laboratory UCS strength of the rock. The alternative form of equation (1) provides good insight, but is rarely used. For this form, assume that the pillar volume is given by $V = w^2h$. The width to height ratio is given by $R = w/h$. When these two equations are inserted in equation (1), it can be expressed in the alternative form:

$$\sigma_p = KV^{(\alpha-\beta)/3}R^{(\alpha+2\beta)/3} \tag{9}$$

For equation (9), if $\alpha = \beta$, it can be seen that the pillar strength is independent of the pillar volume. In contrast, if $\beta > \alpha$, as in the Hedley and Grant formulation, the pillar strength is predicted to decrease as the pillar volume is increased, even if the pillar shape is unchanged (Figure 11).

From the PlatMine research study, it was proposed that for the UG2, K = 67 MPa, α = 0.67 and β = 0.32. A new strength formula was also derived for the Merensky Reef pillars (Watson et al., 2008). For the Merensky formula, K = 86 MPa, α = 0.76 and β = 0.36. For the new UG2 and Merensky pillar strength formulae, note that $\alpha > \beta$. This is in contrast to the Hedley and Grant and Salamon and Munro formulae, where $\alpha < \beta$. The implications of this can be examined by examining equation (9). The pillar strength for the PlatMine Merensky and UG2 formulations, $\alpha > \beta$, will increase as the pillar volume is increased. This is illustrated in Figure 11. It is not clear whether the increase in pillar strength for an increase in volume predicted by the UG2 formula is an appropriate representation of underground pillar strength. Note that the results in the graph are for a cube with a constant width-to-height ratio (R = 1) where only the volume of the cube is increased. It is expected intuitively that as the volume of rock increases, more discontinuities may be present that may weaken the volume of rock.

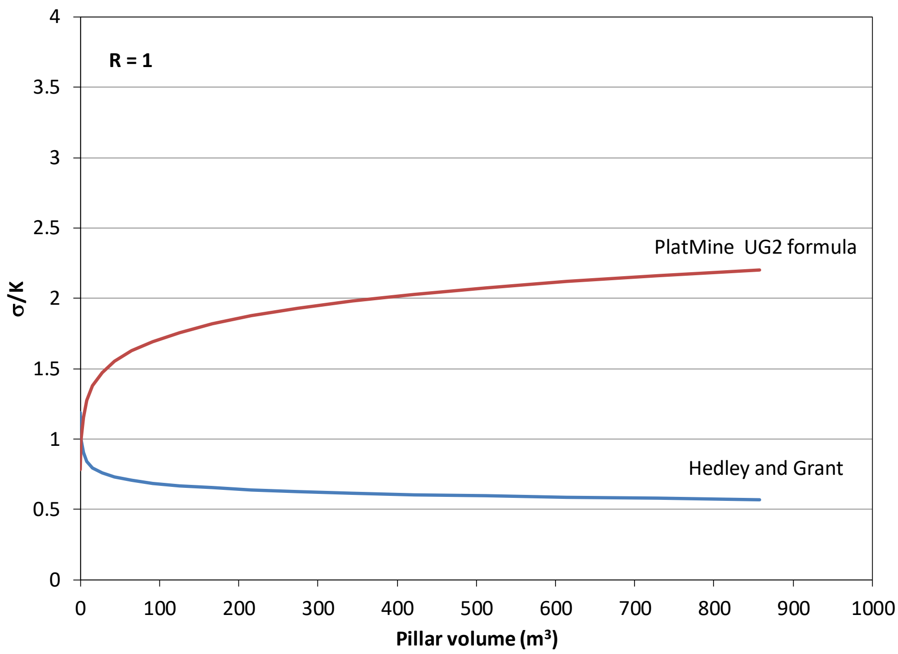

Figure 11. Effect of pillar volume on pillar strength for a constant width to height ratio of 1 (for a cube) (after Malan and Napier, 2021).

4.2 Laboratory experiments to determine appropriate strength formulae

4.2.1 Laboratory experiments on coal specimens

The sections above discussed the early coal experiments that led to the adoption of the power-law formula. Most of this work was based on underground experiments on small pillars. Some additional laboratory experiments on coal specimens are described below for completeness.

Steart (1954) conducted laboratory experiments on small cubes of coal in the laboratory. Unfortunately, he does not describe the experiments and specimen sizes in detail. He published the table in Figure 12 and this was for specimens with a width of 9 inches (≈229 mm). These specimens were tested at four different heights. The coal was sourced from the Durban Navigation Colliery in Natal.

Height inches	Width inches	Total crushing load, tons	Crushing pressure tons per sq. inch
27	9	28·2	·35
18	9	40·8	·50
9	9	78·5	·97
4	9	184·5	2·30

Figure 12. Laboratory experiments on coal published by Steart (1954).

For this current project, the strength data in Figure 1 was plotted as a function of the width to height ratio (w/h) and this is illustrated in Figure 13. The units of strength, "tons per sq. inch", were retained as it is not known if the author of the paper used imperial or metric tons for the measurements. This graph is fascinating as, for these few laboratory measurements, the R^2 value is essentially 1 and therefore there is a very clear linear relationship between the strength and the w:h ratio.

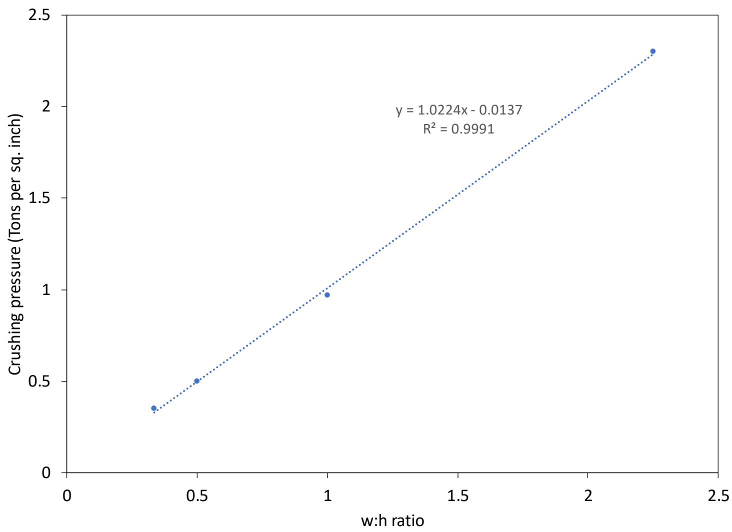

Figure 13. Relationship between strength and w:h ratio based on the laboratory experiments on coal published by Steart (1954).

The effect of specimen height is shown in Figure 14. All the samples had a width of 9 inches and this graph illustrates the decreasing strength for increasing "pillar height".

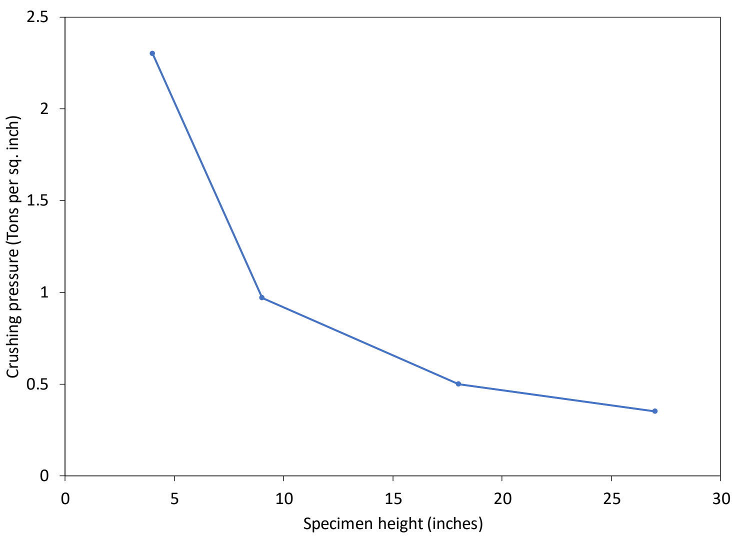

Figure 14. Relationship between strength and specimen height based on the laboratory experiments on coal published by Steart (1954).

As discussed above in Section 4.1.1, Steart (1954) noted that three rules apply to the strength of pillars. Rule 3 is verified by additional data presented below. The interesting rule that requires further scrutiny is Rule 2 (Figure 2). No additional data is given in Steart's paper to verify this. As the specimen height given in Figure 2 is 1, the given width is essentially similar to the w:h ratio. The shape of Figure 2 does not agree with the authors' own plot of his data in Figure 13. The limited laboratory results give a linear trend, whereas Steart assumed the strength was curving downward. The motivation in his paper for the adoption of Rule 2 is therefore not clear and this apparent discrepancy requires further investigation.

Bieniawski (1968a) tested cubical coal specimens with sizes varying from 2 cm to 2 m. Although, these tests were conducted underground, these are analogous to laboratory testing as the sample preparation equipment and a compression testing machine were taken underground. This is illustrated in Figure 15 and the test results are given in Figure 16.

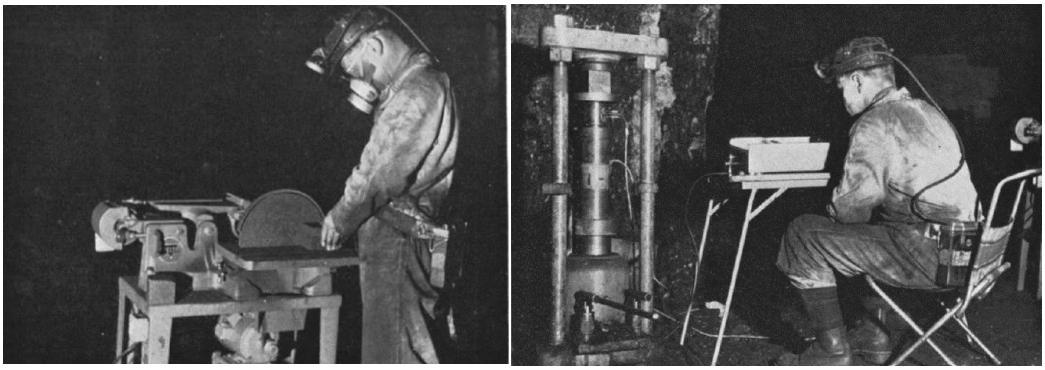

Figure 15. Underground preparation of a small cubical coal specimen (left) and experimental setup for testing these coal specimens (after Bieniawski, 1968a).

Cubic size (in.)	Number off tested	Strength (lb/in²)	Deviation (lb/in²)
0·75	10	4260	814
1	10	4760	700
2	8	4880	1070
2·7	5	4575	1250
3	6	4070	400
6	7	1850	435
12	4	1158	115
18	2	910	12
24	1	800	—
28	1	774	—
36	2	709	2
48	2	650	20
60	2	643·5	20

Figure 16. Experimental test results on coal published by Bieniawski (1968a).

The test results are illustrated graphically in Figure 17. These results are essentially similar to the graph presented by Steart (1954) for Rule 3.

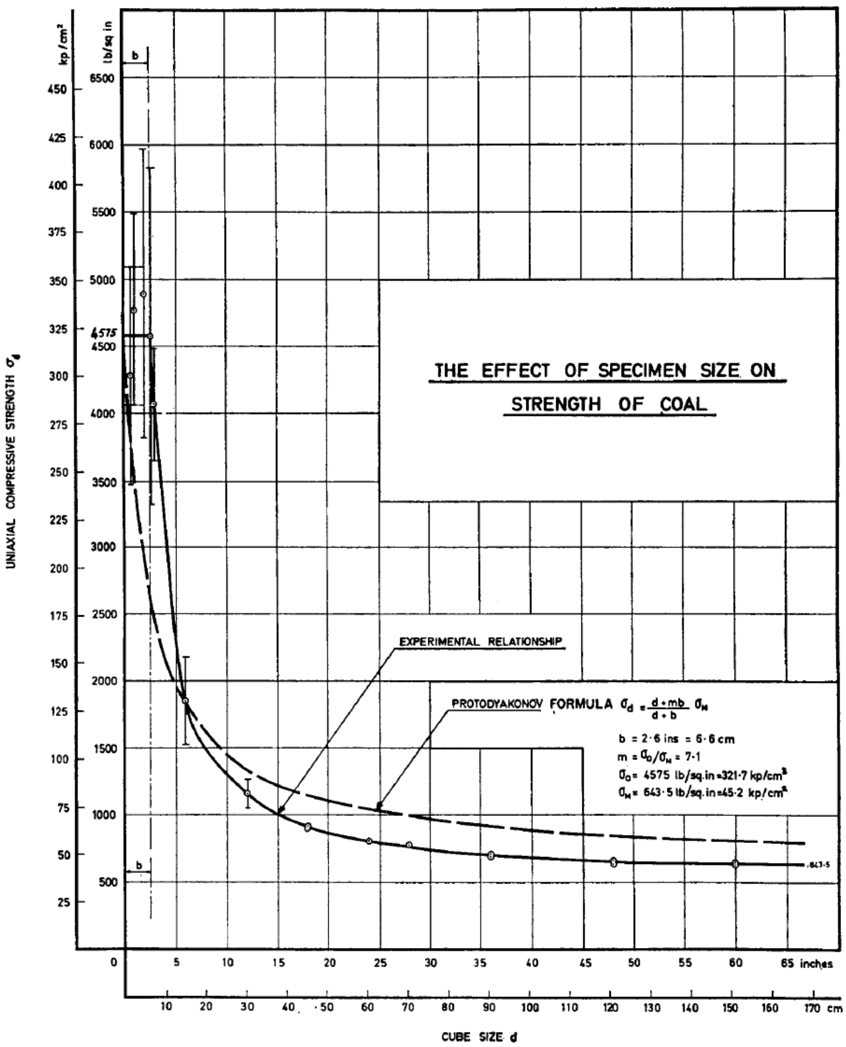

Figure 17. The effect of specimen size on the strength of coal (after Bieniawski, 1968a).

Of interest is that Figure 17 has essentially the same form as Figure 3, but Bieniawski also tested larger cubes and he argued that this gave approximately a constant strength for sizes greater than 5 feet.

From Figure 17, Bieniawski identified two important parts of the curve namely

1. **The strength reduction relationship**
2. **The final constant strength relationship**

This has important implications when choosing an appropriate pillar strength formula and this is where the linear formula for underground pillars was born. He suggested two mathematical relationships to describe the laboratory behaviour in Figure 17.

For part (1):

$$\sigma = 1100\frac{w^{0.16}}{h^{0.55}} \tag{10}$$

For part (2):

$$\sigma = 400 + 220\frac{w}{h} \tag{11}$$

The units of equations (1) and (2) are (lb/in²) where w is the width in feet and h is the height in feet. Equation (2) is valid for coal specimens with sizes larger than 5 feet (1.5 m).

Of particular interest is that Bieniawski recommended two different equations to describe his data, while other workers, as described below, recommended a single power-law function with an exponent of approximately -½ to describe this behaviour. The difficulty with this is that the strength will decrease forever with increasing side length of the cube and possibly for this reason, Bieniawski preferred equation (2) for actual underground pillars.

4.2.2 Laboratory experiments on hard rock

Bieniawski (1968b) also published results on the testing of cubes of norite. The results are shown in Figure 18. Note that the strength appears to become constant for specimen sizes larger than 125 mm.

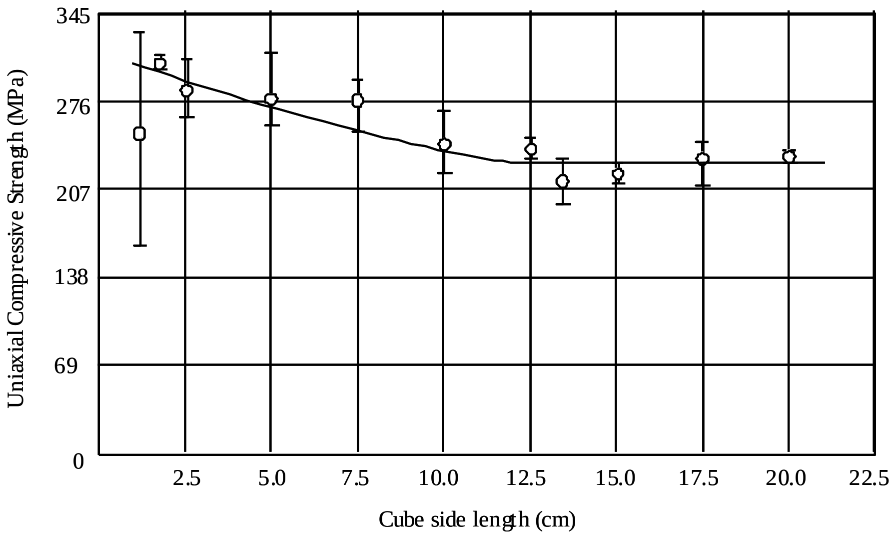

Figure 18. The effect of specimen size on the strength of norite specimens (Bieniawski, 1968b).

Bieniawski's data was presented in a different format by Celik (2017) who fitted an exponential decay function to the data (Figure 19).

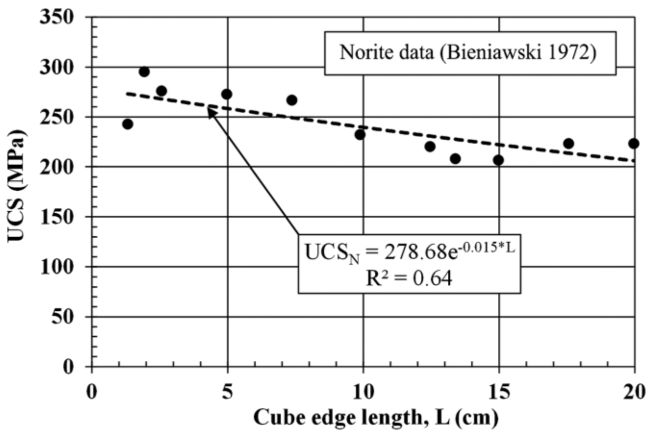

Figure 19. The effect of specimen size on measured UCS values of norite (after Celik, 2017).

Heuze (1980) published the graph shown in Figure 20 of iron ore and diorite to illustrate that the size effect nearly disappears when the volume of rock reaches 1 m^3. This is supports Bieniawski's hypothesis given above. When planning a laboratory testing programme, it is therefore important to make provision for large specimens.

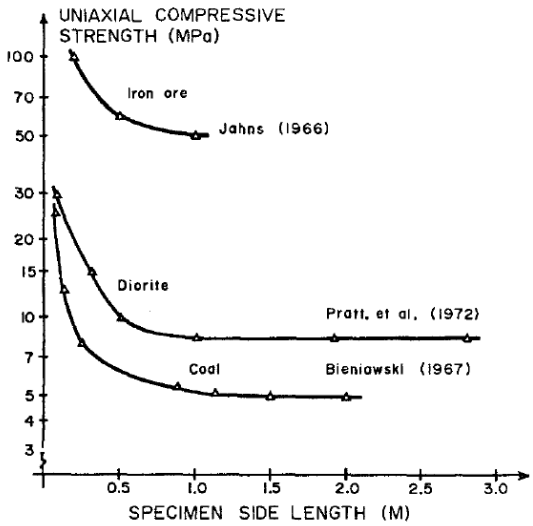

Figure 20. Effect of specimen size on measured uniaxial compressive strength of coal and iron ore (after Heuze 1980).

More data from Pratt et al (1972) on diorite tests are shown in Figure 21. A similar trend is seen for this data compared to that given in Figure 20.

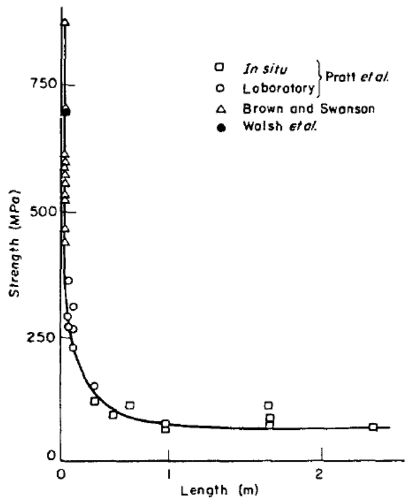

Figure 21. Effect of specimen size on measured uniaxial compressive strength of diorite (after Pratt et al, 1972).

Hustrulid (1976) suggested in his analysis of Bieniawski's and other coal data that a power law of exponent -½ would correctly predict the strength decay with cube edge length (Figure 22). However, such a law will eventually predict vanishing strength as the size increases further and this is not realistic. This is an aspect that motivated Bieniawski (1968) to propose a linear pillar strength formula.

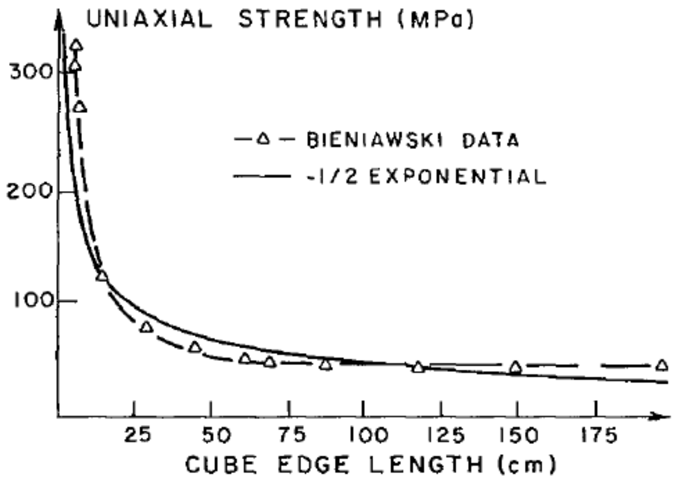

Figure 22. Effect of specimen size on measured uniaxial compressive strength of diorite (after Pratt et al, 1972).

York and Canbulat (1998) published results from the testing of Merensky Reef from Amandelbult Mine and the results are shown in Figure 23. Similar to the work by Bieniawski, they note that the size effect dies out beyond a critical size (also see Ryder and Jager, 2002). They estimated that this occurs at a specimen size of approximately 150 mm. This is much smaller than the 1.5 m size for coal specimens obtained by Bieniawski (1968a).

The line fitted in Figure 23 can be questioned, however, as there is a large scatter in the data and only two tests were conducted for the 250 mm specimen sizes.

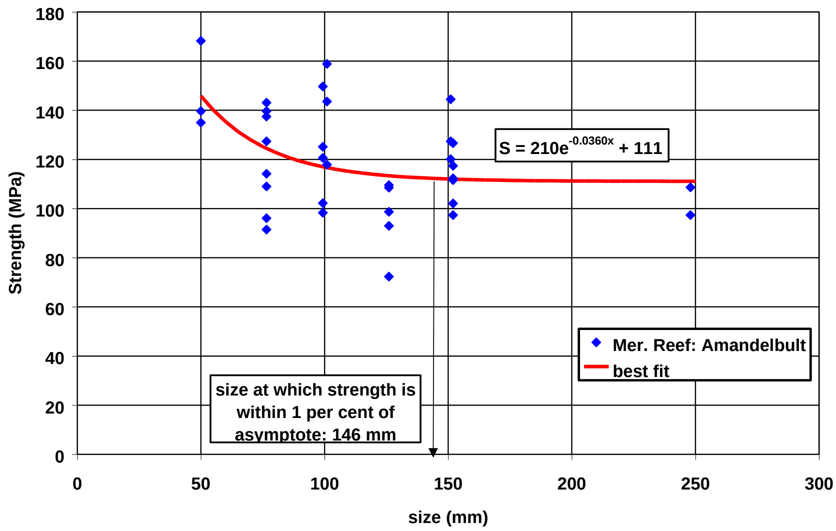

Figure 23. The effect of specimen size on the strength of Merensky Reef specimens (after York and Canbulat, 1998, also published in Ryder and Jager, 2002).

Celik (2017) investigated the effect of cubic specimen size on uniaxial compressive strength of carbonate rocks from Western Turkey. He summarised the results of previous workers as shown in Figure 24.

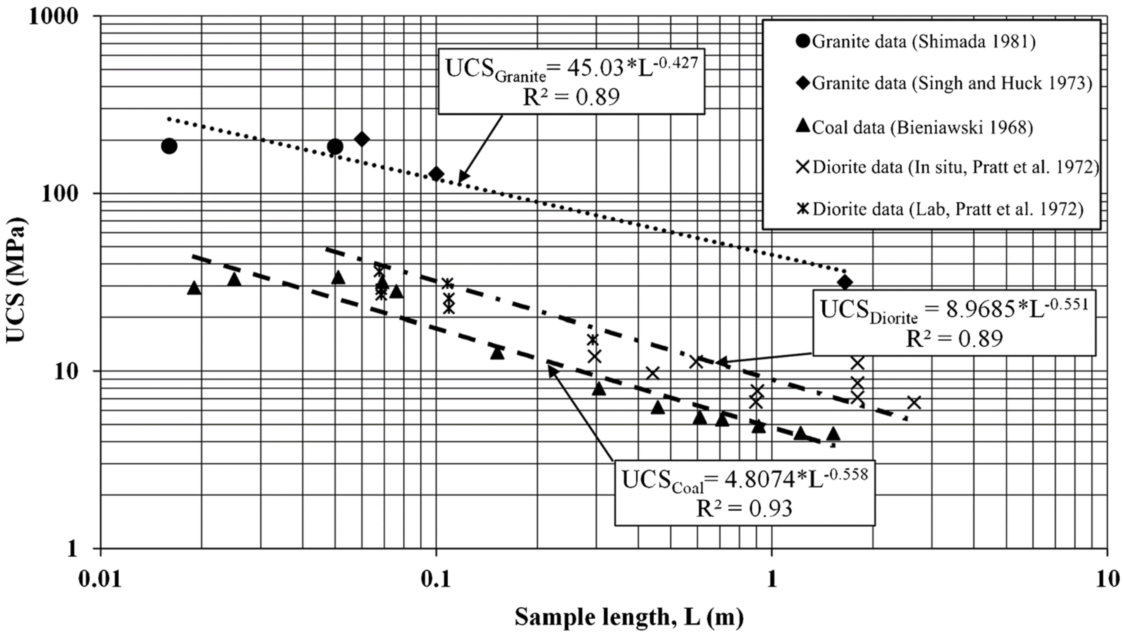

Figure 24. The effect of specimen size on the UCS values for some rocks (after Celik, 2017).

Note that the data in Figure 24 seems to illustrate that the Uniaxial Compressive Strength (UCS) of the cubes decrease with side length, L, according to a power-law of the form:

$$UCS = CL^{-\gamma} \tag{12}$$

where C is a constant dependent on the rock type and γ is a constant with a value between 0.4-0.6 (see Figure 24) and Hustrulid (1976) suggested it should be 0.5. Based on equation (12), for large sample sizes, $L \gg$, only small changes in strength is noted for changes in L. The drawback of equation (12) is that in the limit when $L \to \infty$, then $UCS \to 0$. If $\gamma = 0.5$, then equation (12) can be written as:

$$UCS = CL^{-0.5} = \frac{C}{\sqrt{L}} \tag{13}$$

This confirms the third rule from Steart (1954) that the strengths of pillars, with the shape of a cube, vary in inverse ratio to the square root of their dimensions. This is also shown in Figure 22 (plotted on a linear axis and not a logarithmic axis).

Celik (2017) conducted additional testing on limestone type rocks and Figure 25 illustrate his testing equipment. His test results are given in Figure 26 and the power-law given in equation (12) again gives a good fit.

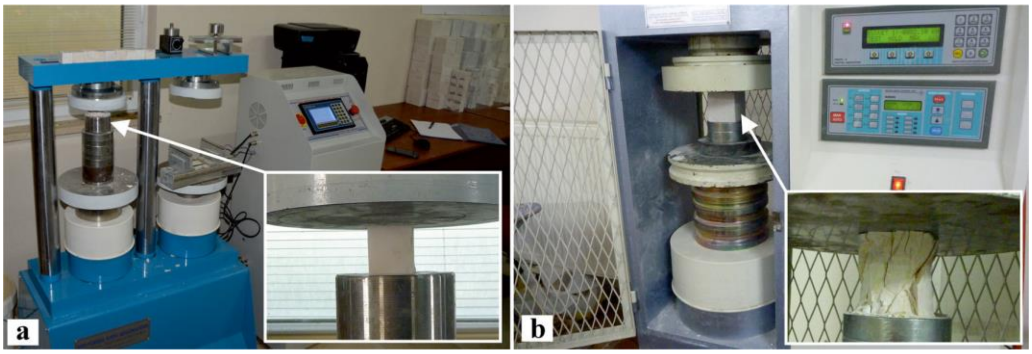

Figure 25. Testing equipment to investigate the effect of specimen size on Limestone rocks (after Celik, 2017).

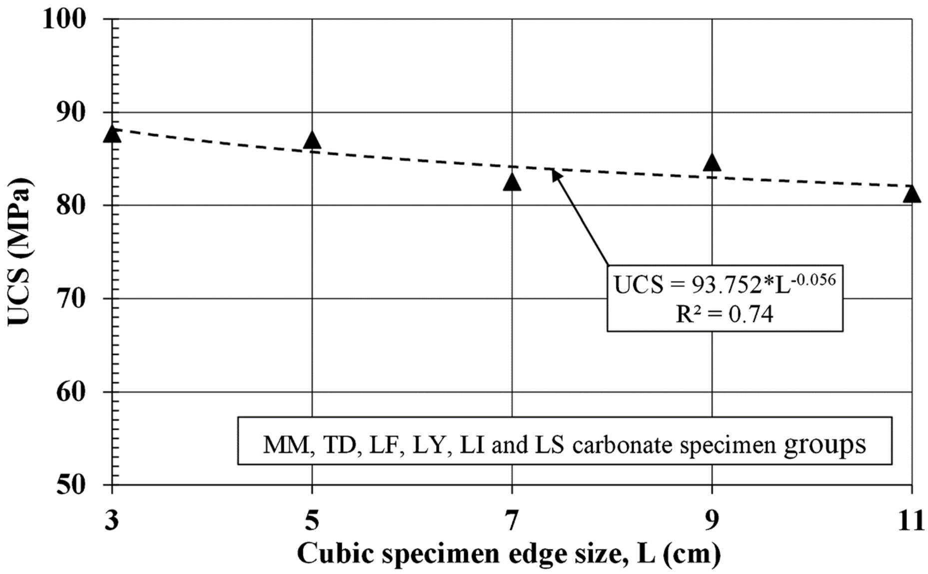

Figure 26. UCS decreasing with increasing specimen size for five carbonate rock groups (after Celik, 2017).

4.2.3 Discussion on the power-law strength formula in relation to the laboratory results

A key aspect of the project is to gain an improved understanding of the most appropriate formula to use for pillar strength. The discussion above indicated that the laboratory results on cube specimens do indeed follow the third rule of Steart (1954) namely that the strengths of pillars in cube form vary in an inverse ratio to the square root of their dimensions.

For a pillar with the shape of a cube, $w = h$, and therefore equation (1) can be written as:

$$\sigma_p = K\frac{w^\alpha}{w^\beta} = Kw^{\alpha-\beta} \tag{14}$$

The third rule of Steart (1954), verified from the laboratory data above, therefore implies that the following condition must be true:

$$\alpha - \beta = -0.5 \tag{15}$$

Interestingly, the current exponents of both the Hedley and Grant and Salamon and Munro formulae does not meet the criterion in equation (15).

Furthermore, equation (15) will be satisfied is $\alpha = 0.5$ and $\beta = 1$. This will imply a strength formula of the form:

$$\sigma_p = K\frac{w^{0.5}}{h} \tag{16}$$

This also satisfies Steart's first rule, namely that the strengths of pillars of the same width vary in inverse ratio to their height, as well as the second rule that the strengths of square pillars of the same height varies as the square root of their widths. Figure 27 is included to illustrate the effect of the height parameter if different exponents are used in the power-law formula. The Hedley and Grant equation is compared to equation (16). Equation (16) is more sensitive to an increase in height and a larger relative reduction in pillar strength is experienced for greater pillar heights. For equation (16), the strength for a pillar height of 2.5 m is 60% of the strength at a height of 1.5 m, whereas it is 68% for the Hedley and Grant formula.

Although equation (12) and possibly equation (16) may be applicable to laboratory sized specimens, the application of the power-law formula in equation (16) is unclear and Bieniawski's suggestion of a linear pillar formula for pillar sizes in the order of several metres may be appropriate. This needs to be investigated in future.

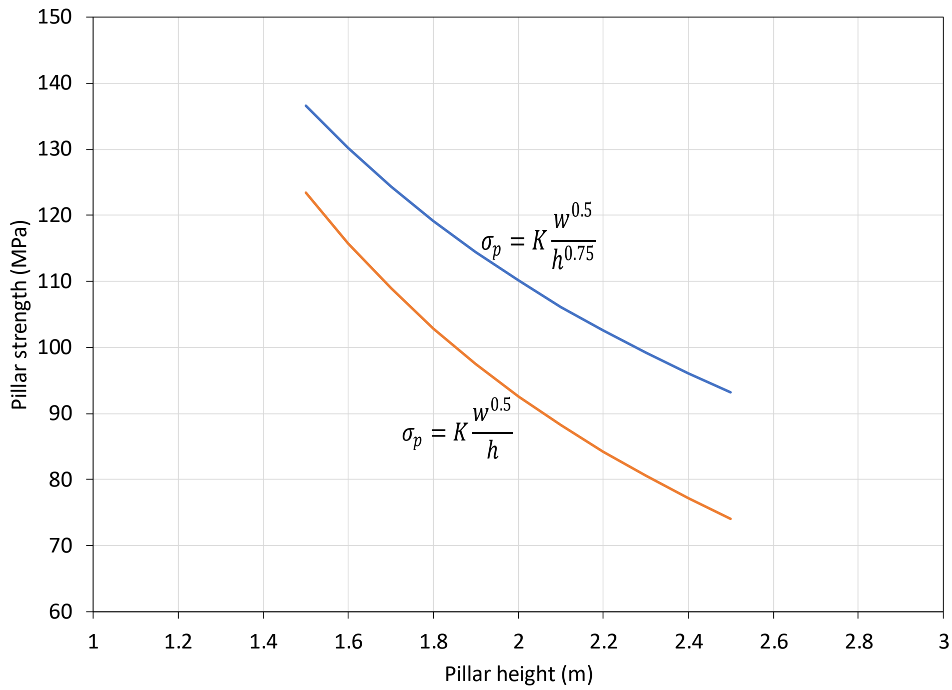

Figure 27. Comparison of two different power-law strength formulae and the effect of the height parameter. These graphs were plotted for $w = 7\ m$ and $K = 70\ MPa$.

4.3 Insights from numerical and analytical modelling

4.3.1 Previous numerical modelling of the effect of width to height ratio

Martin and Maybee (2000) conducted two-dimensional finite element modelling (Phase2 code) with a Hoek and Brown failure envelope in an attempt to replicate the empirically observed pillar behaviour. The Hoek-Brown failure envelope includes a cohesive strength component and a stress-dependent frictional component providing confinement. For pillars with width to height ratios greater than 1, the frictional strength component increases rapidly. They found that by using conventional Hoek and Brown parameters for typical hard-rock rib-pillars, the modelling results predicted pillar-failure envelopes that did not agree with the observed empirical failure envelopes. It seems that for pillar width-to-height ratios less than 1.5, the strength of the hard-rock pillars is fundamentally controlled by a loss of cohesion and the frictional strength component can be ignored. Their modelling with modified Hoek and Brown “brittle parameters” predicted pillar strength curves that were in better agreement with the observed empirical failure envelopes (Figure 28). Note that the empirical strength curves are downward sloping while the numerical curves slope upwards for increasing width to height ratios.

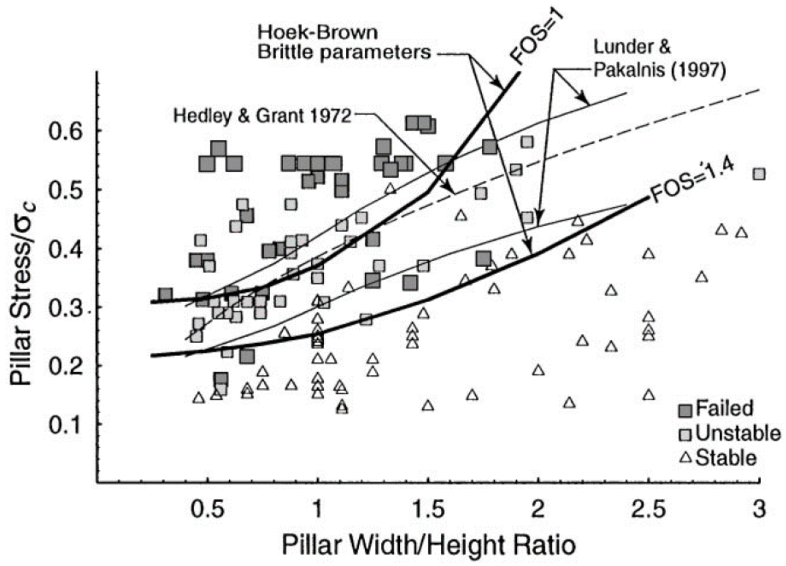

Figure 28. A comparison of the empirical pillar strength curves and the Phase2 modelling results using Hoek and Brown brittle parameters (after Martin and Maybee, 2000).

Esterhuizen (2014) conducted modelling to investigate if the numerical models can simulate the effect of width-to-height ratio on pillar strength. Model calibration and validation were carried out against the empirically developed pillar design method of Roberts et al. (2007) as well as the Lunder and Pakalnis (1997) pillar strength equation for hard rock pillars. Models were created to simulate pillars with width to height ratios of 0.5 to 2.0 and the results were compared to the empirically developed equations. The program used was the two-dimensional code UDEC. The rock mass properties were selected to simulate a good quality rock mass representative of the rock found in limestone mines.

Figure 29 illustrates the comparison between the empirical and modelling results. It was concluded by Esterhuizen (2014) that the modelling method provides a realistic representation of pillar strength over the range of width-to-height ratios shown. The "semi-empirical" equation he used for the curve in Figure 29 is the one given by Roberts et al. (2007) and is referred to as the confinement formula:

$$P_s = (K \times UCS)(C_1 + C_2\kappa) \tag{17}$$

where

P_s = pillar strength

K = pillar strength size

C_1, C_2 = empirical rock mass constants

κ = pillar friction term

UCS = unconfined compressive strength

Furthermore

$$\kappa = tan\left\{cos^{-1}\left[\frac{1-C_{pav}}{1+C_{pav}}\right]\right\} \tag{18}$$

where

C_{pav} = average pillar confinement

The parameter C_{pav} was derived from two-dimensional modelling of a pillar of varying widths to heights. The following equation was adopted for these numerical modelling results:

$$C_{pav} = Coeff \times \left[Log\left(\frac{w}{h} + 0.75\right)\right]^{\frac{1.4}{(w/h)}} \tag{19}$$

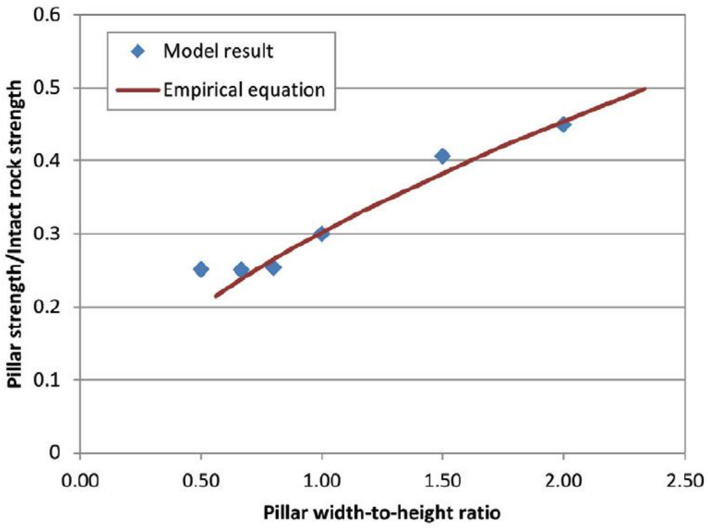

Figure 29. Comparison of the UDEC model results of a pillar and the pillar strength equation given in Roberts et al. (2007)

A good fit is seemingly obtained in Figure 29 between the numerical models and the empirical strength formula, although it can be argued that a much simpler power-law or linear formula may give an equally good fit. The complexity of the confinement formula makes it less attractive for everyday use. Furthermore, at higher width to height ratios, the numerical modelling may have even predicted an increasing slope for the curve, which cannot be simulated by the empirical strength equation of Roberts et al. (2007).

An important point to emphasise is that on the strength versus width to height diagrams for the empirical power-law equations (Figure 28), the curves have a "downward increasing concave" shape for increasing pillar width to height ratios. The implication of this is that these equations cannot simulate the transition to much stronger squat pillar behaviour at very large width to height ratios. Another objection raised by Bieniawski (1992) is that, according to the power-law formulation, the cube strength (w = h) would continue to decrease indefinitely with side length. This is considered unreasonable (Hustrulid, 1976). The numerical modelling in Figure 28 illustrates a different pillar strength behaviour, however, and it is "upward increasing concave" when using the Hoek and Brown brittle parameters in Phase2. Martin and Maybee (2000) did not specifically refer to the shape of their curves and that it is upward concave. According to the best knowledge of the authors, this focus on the upward and downward curves is emphasised for the first time in this Samerdi project.

4.3.2 Analytical modelling of the effect of width to height ratio

To obtain further insight into the strength of pillars, it was worthwhile to investigate the behaviour predicted by an analytical limit equilibrium model. Such a model is implemented in the TEXAN code and has been used extensively to simulate pillar failure behaviour in tabular stopes (Napier and Malan, 2021). The section below considers analytical solutions of this limit equilibrium model and it is not numerical modelling results. The same results can, however, be obtained from TEXAN.

Napier and Malan (2021) derived analytic models of pillar failure for an infinitely long rib pillar and a square pillar, if it behaves according to the assumptions of the limit equilibrium model (Figure 30).

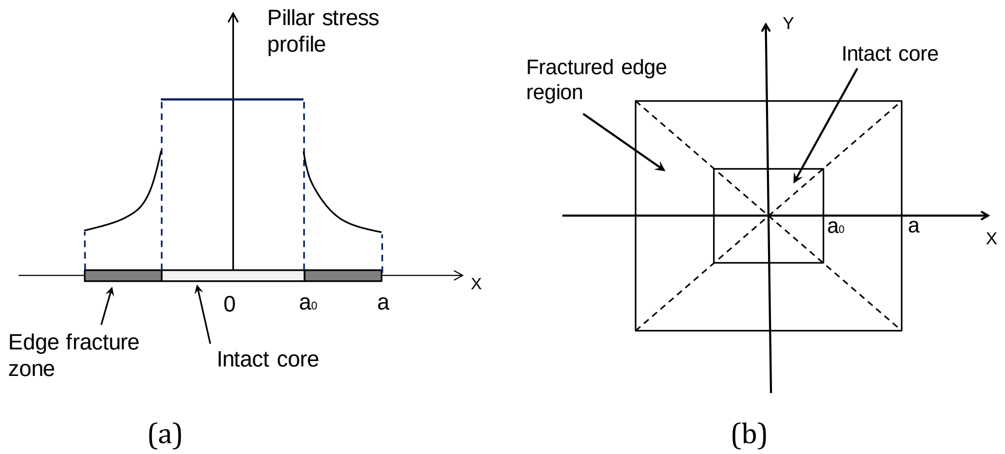

Figure 30. (a) Section view through a rib pillar. The pillar stress profile for a partially failed pillar is shown. (b) Plan view of a square pillar with the intact core shown (after Napier and Malan, 2021).

A limit equilibrium model is assumed for the two pillar shapes shown in Figure 30. The width of the square pillar and the minimum width dimension of the strip pillar is $w = 2a$. The fracture zone on the edge of the pillar is in a state of equilibrium and the vertical extent of the fracture zone is bounded by parting planes at the contacts with the hangingwall and footwall. Using this assumption and a failure model for the reef material, the scaled average pillar stress when the pillars are completely fractured through is given by the following equations (Napier and Malan, 2021).

For a rib pillar:

$$\frac{\bar{\sigma}_n}{\sigma_c} = \frac{(e^{\beta}-1)}{\beta} \qquad (20)$$

For a square pillar:

$$\frac{\bar{\sigma}_n}{\sigma_c} = \frac{2}{\beta^2}\left(e^{\beta} - \beta - 1\right) \qquad (21)$$

and

$$\beta = \frac{mtan\phi_I w}{h} = mtan\phi_I R \qquad (22)$$

where $R = w/h$ is the width to height ratio, ϕ_I is the friction angle at the interfaces of the pillar and the host rock, m is the slope in the residual limit equilibrium strength envelope and σ_c is the intact rock uniaxial strength.

Napier (2018) noted that for the rib pillar, equation (20), as $\beta \to 0$, $\bar{\sigma}_n / \sigma_c \to 1$ and it is apparent that $\bar{\sigma}_n / \sigma_c \to \infty$ exponentially as $\beta \to \infty$. It can be shown that the second derivative $d^2\bar{\sigma}_n / d\beta^2 > 0$ when $\beta > 0$ and consequently that $d^2\bar{\sigma}_n / dR^2 > 0$ when $R > 0$. The pillar strength therefore "accelerates" as a function of the width to height ratio, R. This is plotted in Figure 31. Equation (21) has the same asymptotic behaviour as equation (20) but the average strength is lower.

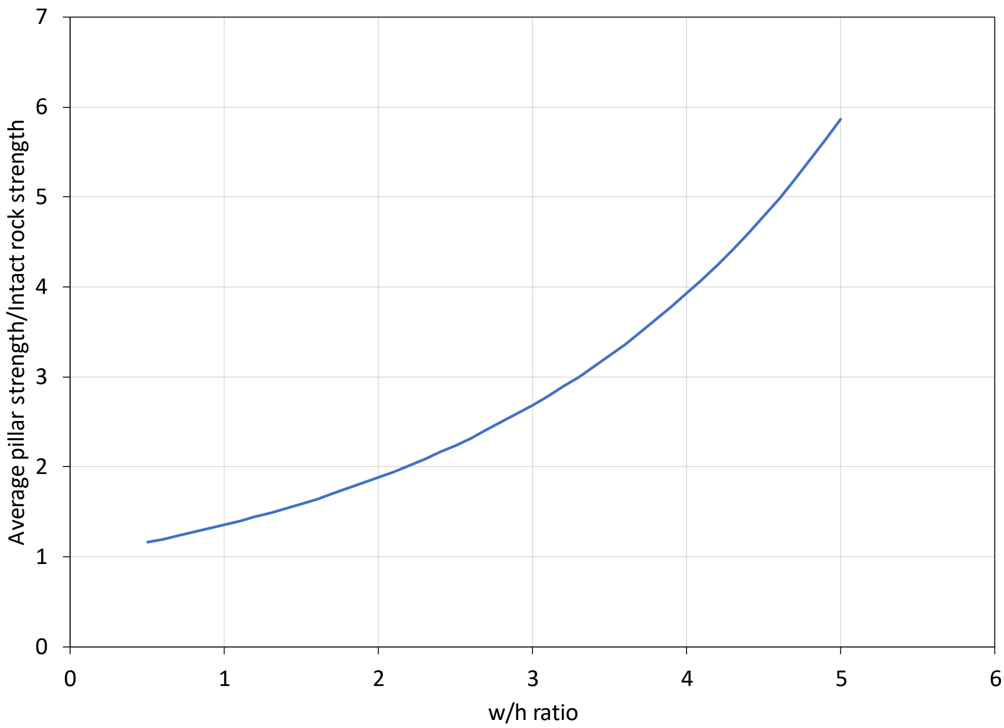

Figure 31. "Accelerating" increasing pillar strength as a function of the width to height ratio (w/h) predicted by the limit equilibrium model.

The accelerating slope behaviour (i.e. $d^2\bar{\sigma}_n / dR^2 > 0$) of the average pillar strength as a function of the pillar width to height ratio, $R = w/h$, predicted by equation (20) and equation (21), does not conform to the strength profiles predicted by empirical power-law strength relationships such as that of Salamon and Munro (1967) where:

$$\bar{\sigma}_n = 7.176\frac{w^{0.46}}{h^{0.66}} \quad MPa \tag{23}$$

Equation (23) applies to square pillars and can be expressed in terms of the pillar volume, $V = w^2h$, and the width to height ratio, $R = w/h$ as:

$$\bar{\sigma}_n = k\frac{R^{\eta}}{V^{A}} \tag{24}$$

with $k = 7.176$ MPa, $\eta \approx 0.5933$ and $A \approx 0.06667$. Differentiating equation (24) twice with respect to R yields:

$$\frac{\partial^2\bar{\sigma}_n}{\partial R^2} = \frac{-k\eta(1-\eta)}{R^{2-\eta}V^{A}} \tag{25}$$

which is negative when $0 < \eta < 1$.

A so-called "squat pillar" adaptation of equation (24) has been proposed by Madden (1991) where it is suggested that equation (24) should be modified when the width to height ratio R exceeds a critical limit R_0. The squat pillar strength relationship consequently resembles the strength shape that is predicted by equation (20) or by equation (21).

It is apparent that the major differences between many empirical pillar strength relationships are characterised by the evolution of the pillar strength curvature, represented by the sign of the second derivative as a function of the pillar width to height ratio, R. Additional work not discussed in this report indicated that the limit equilibrium model, with a spalling transition region, can replicate the behaviour of empirical formulas for pillar strength, including the transition to so-called "squat" pillar behaviour (Napier, 2018). This seems to be an attractive model to simulate the observed pillar strength as a function of the width-to-height ratio.

4.3.3 FLAC3D modelling of the effect of width to height ratio

The Phase2 and UDEC modelling described in Section 4.3.1 are two-dimensional codes and the work therefore simulated infinitively long rib pillars. It was attempted to extend the work for this project by simulating a three-dimensional pillar at different width to height ratios. The FLAC3D (Fast Lagrangian Analysis of Continua) code was used for this. This code was developed by ITASCA Consulting for the analysis of geotechnical problems. It has the capability of modelling both elastic and a large variety of complex non-linear behaviours.

The FLAC3D code is based on the finite difference method. This method is often considered a subset of the finite element method where the entire problem space needs to be covered by a mesh of elements. Similar to other modelling approaches, the finite difference method only provides an approximation of the solution to the problem. This method is frequently used to model rock masses of different strengths. One of the unique strengths of FLAC is its ability to simulate materials that undergo large deformations and plastic flow when yielding. FLAC3D is a three-dimensional version of the FLAC software that is able to model soil, rock and backfill behaviour, including plastic failure, using a representative finite difference grid.

The pillar problem was simplified and a single three-dimensional pillar was considered. (Figure 32). The width to height of this pillar was changed in an attempt to replicate the curves obtained from the two-dimensional modelling illustrated above.

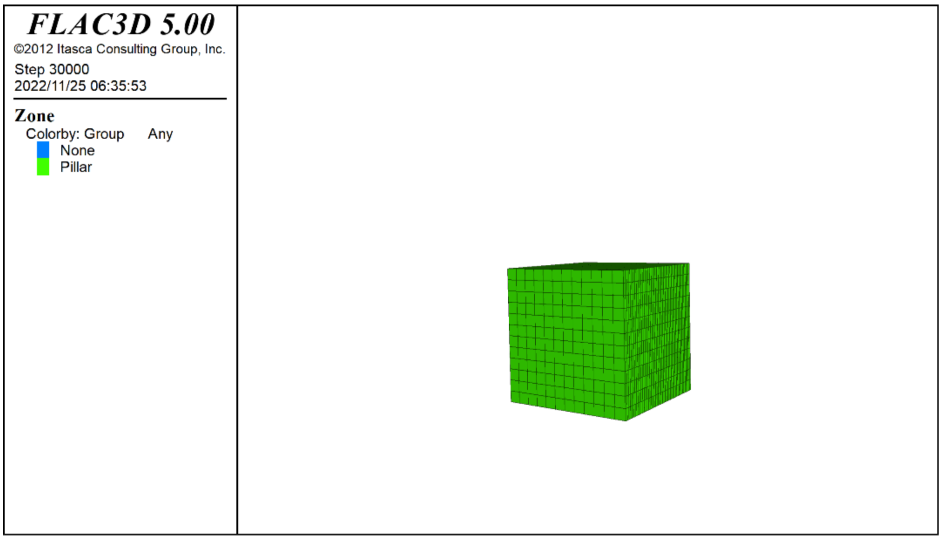

Figure 32. An illustration of a pillar simulated with a width to height ratio of 1.

The input parameters used for the numerical modelling study include rock mass properties, geometry of the pillar and also the loading conditions. The numerical model was subjected to a constant loading velocity in the vertical direction for the period when the rock was intact. A shear strength envelope for rock mass should be used to simulate failure. The most popular methods to simulate the inelastic behaviour are to use the Mohr-Coulomb or the Hoek Brown constitutive models.

For simplicity, the Mohr-Coulomb constitutive model without allowing any strain softening was used. This failure criteria enabled the determination of a peak strength for the different pillar geometries. Table 2 illustrates the parameters used for the simulations.

Table 2. Parameters used in the FLAC3D model.

Input parameter	Value
Deformation modulus (GPa)	27.8
Poisson's ratio	0.25
Density (kg/m^3)	2750
Cohesion (MPa)	0.25
Friction angle (degrees)	33
Tensile strength (MPa)	0.019

Figure 33 illustrates the development of a failure plane in the model.

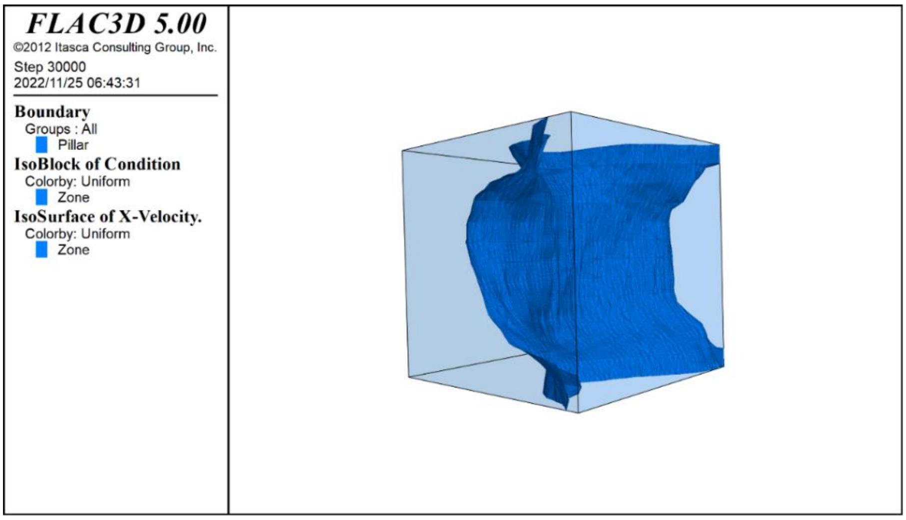

Figure 33. An illustration of one of the first failure planes in the pillar. This is reminiscent of the hourglass failure pattern often seen underground and for laboratory testing specimens.

A typical simulated load-deformation curve is shown in Figure 34. Note the effect of the Mohr-Coulomb constitutive model without strain softening. There is no significant decrease in stress after the peak strength as the model simulates perfectly plastic failure behaviour. It was evident that a slow loading rate should be used for these models, otherwise spurious results will be obtained (Figure 35). It was also found that the modelling results are extremely sensitive to the imposed boundary conditions and the results obtained from this type of modelling should therefore be treated with caution.

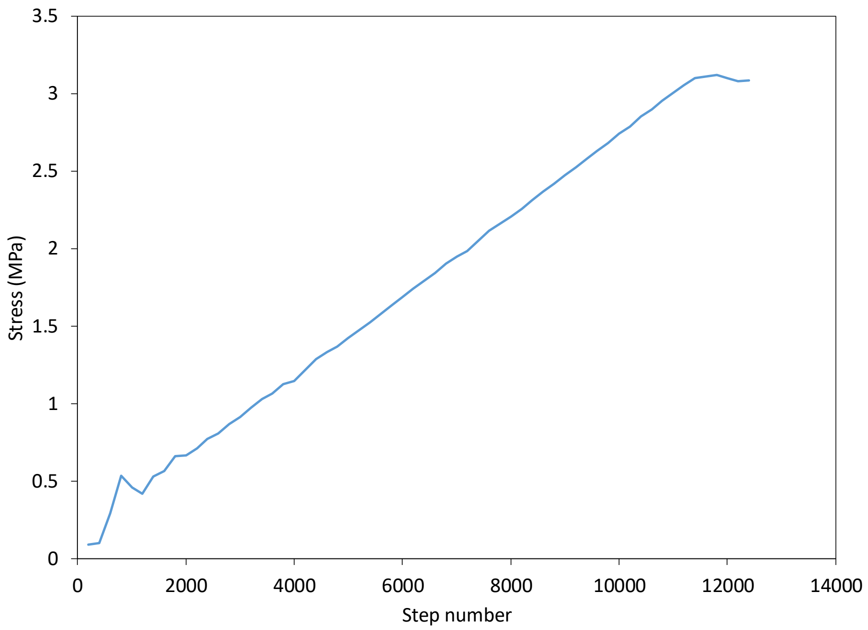

Figure 34. Pillar strength simulation for a pillar width to height ratio of 0.8.

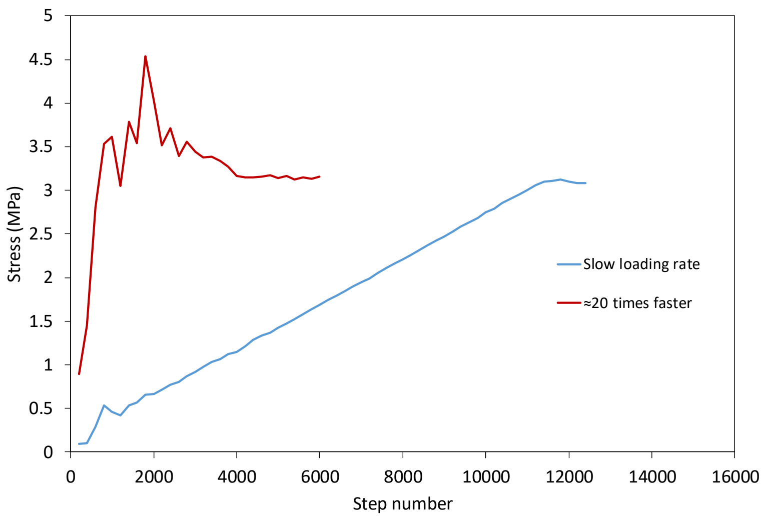

Figure 35. Effect of loading rate on load-deformation behaviour of the pillar. This is graph is included to illustrate that the FLAC3D models are typically very sensitive to the imposed boundary conditions.

The objective of the modelling was to produce the graph in Figure 36. The simulated peak pillar strength was normalised to the initial rock strength. Interestingly, the curve is "downward increasing concave" similar to the empirical strength curves and contradicts the two-dimensional modelling done by other workers as well as the limit equilibrium model. The reason for this is not clear at this stage and further work needs to be done. This type of modelling seems to be sensitive to the type of failure model selected as well as the imposed boundary conditions and no further modelling work was therefore done for this project.

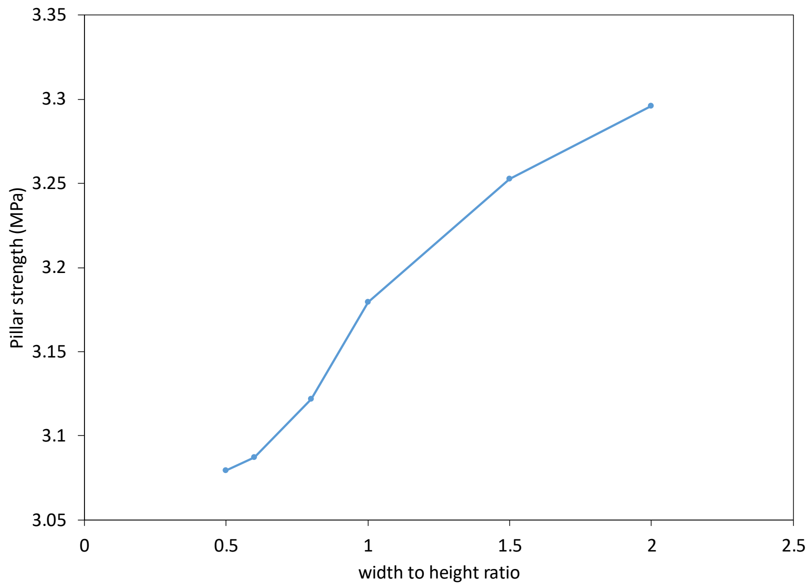

Figure 36. Comparison of the simulated pillar strength as a function of width to height ratio.

5 DISCUSSION

5.1 Results Summary

One of the most important findings from this study is that, in the global rock engineering fraternity, there is significant uncertainty regarding the most appropriate pillar strength formula to use. To highlight this aspect, Table 3 illustrates the large number of pillar strength formulae developed for the coal mining industry alone. Examples of the various formulae developed for the hard rock industry were also given in Table 1 (Section 4.1.4). Table 3 is included in this report as it subtly gives important insight into the recommended future research direction. It may simply not be the best option to spend significant resources to develop yet another formula. It is surprising that every research study proposed a different pillar strength formula to fit the newly collected data. It seems very difficult to find a "universal" pillar formula. The reason for this can possibly be found in the variability of the rock mass strength, the different pillar failure mechanisms, not considering the stiffness of the loading system and the uncertainty in terms of the in-situ stresses. Experimental errors may also contribute to the problem. This uncertainty and the lack of historic success present a daunting problem. A different approach is therefore recommended in this report that may possibly benefit the industry more in the short term.

Table 3. A listing of the large number of pillar strength formulae developed for coal pillars (Das et al. 2019).

Table 1 Various coal pillar strength formulae

Sl no.	Authors	Equation	How derived	Slender/ squat pillar	Kind of strength employed
1	Greenwald et al. (1941)	$s = 0.67k\frac{w^{0.5}}{h^{0.88}}$	In-situ test	Slender	In-situ size 30 cm
2	Gaddy (1956) Holland (1964)	$s = k\frac{w^{0.5}}{h}$	Lab test	Slender	Lab size 25 mm
3	Obert and Duval (1967)	$s = k\left(0.78 + 0.22\frac{w}{h}\right)$	Lab test	Slender	In-situ size 'critical'
4	Salamon and Munro (1967)	$s = 7.2\frac{w^{0.46}}{h^{0.66}}$	Pillar cases	Slender	Constant strength
5	Salamon and Munro (generalised)	$s = 0.79k\frac{w^{0.46}}{h^{0.66}}$			In-situ size 30 cm
6	Bieniawski (1968)	$s = k\left(0.64 + 0.36\frac{w}{h}\right)$	In-situ test	Slender	In-situ size 'critical'
7	Bieniawski (modified) Logie and Matheson (1982)	$s = k\left(0.64 + 0.36\frac{w}{h}\right)^{1.4}$		Squat	In-situ size 'critical'
8	Salamon and Wagner (1985)	$s = 0.79k\frac{R^{0.46}}{V^{0.66}}\left\{\frac{0.59}{\varepsilon}\left[\left(\frac{R}{R_0}\right)^{\varepsilon} - 1\right] + 1\right\}$ where, R_0 = critical w/h = 5, R = w/h of pillar, V = pillar volume, ε = a constant = 2.5 (proposed)	Case studies and theoretical analysis	Squat	In-situ size 30 cm
9	Wilson (1972)	*Case I* $w > 2\bar{x}$ (All equations of Wilson are in tonne, ft unit) *Rectangular pillar* $s = \frac{4\gamma H}{w_1 w_2}\left[\begin{array}{l} ww_1 - 1.5(w + w_1)hH \times 10^{-3} \\ +3h^2H^2 \times 10^{-6} \end{array}\right]$ *Long pillars* $s = \frac{4\gamma H}{w}\left(w - 1.5hH \times 10^{-3}\right)$ *Case II* $w \leq 2\bar{x}$ *Rectangular pillar* $s = 667\gamma\frac{w}{w_1 H}\left(w_1 - \frac{w}{3}\right)$ *Long pillars* $s = 667\gamma\frac{w}{H}$ $\bar{x} = 0.0015hH$ is the failed coal zone $\gamma = 0.0707$ t/ft^2 is the rock density	Theoretical analysis	Both	No strength
10	Wilson (1983)	*Case I* Roadways stable $s = \frac{1}{ww_1}\int_{qp}^{q\gamma H}(w - 2x)(w_1 - 2x)d\sigma + qp$ $+ \frac{\sigma_0}{ww_1}(w - 2\bar{x})(w_1 - 2\bar{x})$ *Case II* Roadways unstable $s = \frac{1}{ww_1}\int_{qp}^{\sigma'}(w - 2x)(w_1 - 2x)d\sigma + qp$ where $\sigma' = qp\left(\frac{w}{h} + 1\right)^{q-1}$ or $qp\exp\left(\frac{wF}{2h}\right)$ σ_0 = *in-situ* strength, p = a constant for broken coal = 0.1 MPa (suggested), q = triaxial constant = 3.5 (average suggested) These equations are subject to the following two ground conditions (1) Yield in roof, seam, and floor $x = \frac{h}{2}\left[\left(\frac{\sigma}{qp}\right)^{1/(q-1)} - 1\right]; \bar{x} = \frac{h}{2}\left[\left(\frac{\gamma H}{p}\right)^{1/(q-1)} - 1\right]$ (2) Yield in seam, rigid roof, and floor $x = \frac{h}{F}\ln\frac{\sigma}{qp}; \bar{x} = \frac{h}{F}\ln\frac{\gamma H}{p}$ where $F = \frac{q-1}{\sqrt{q}} + \frac{(q-1)^2}{q}\tan^{-1}\sqrt{q}$ ($\tan^{-1}$ in radians)	Theoretical analysis	Both	In-situ strength = (lab. Strength)/5
11	Sheorey et al. (1986)	$s = 0.66kh^{-0.35} + 6.3\left\{K\gamma H\left[1 - \exp\left(-\frac{1.5w}{D}\right)\right]\right\}^{0.8}$ where $D = 25 + 0.1\ H$, K = virgin horizontal–vertical stress ratio	Theoretical, empirical method, and case study	Both	In-situ size 30 cm
12	Sheorey et al. (1987)	$s = 0.27k\frac{w^{0.5}}{h^{0.86}}$	Case studies	Slender	Lab size 25 cm
13	Sheorey et al. (1987)	$s = 0.27kh^{-0.36} + \frac{H}{160}\left(\frac{w}{h} - 1\right)$	Theoretical, empirical method, and case study	Both	Lab size 25 cm
14	Sheorey (1992)	$s = 0.27kh^{-0.36} + \left(\frac{H}{250} + 1\right)\left(\frac{w}{h} - 1\right)$	Theoretical, empirical method, and case study	Both	Lab size 25 cm
15	Vander Merwe (1999)	$s = 4\frac{w^{0.81}}{h^{0.76}}$	Case studies		Constant strength
16	Vander Merwe (2003a)	$s = k\frac{w}{h}$ (k = 2.8–3.5)	Case studies		Constant strength

As stated above, a key aspect of this study was to test the hypothesis of whether a linear formula may be better suited to describe the pillar strength in the South African mines compared to a power-law formula. It is concluded that there is still uncertainty in terms of this aspect after the study and both the power-law and linear formulae and variations of these are used freely. Perhaps the most insightful is the work by Bieniawski (1977) which indicated that a linear formula is equally as good to represent the coal strength compared to the more commonly used Salamon power-law formula (Figure 37). There is simply not enough evidence to state that one formula is better than the other. This is further highlighted in Figure 38. For the survey of the full-size coal pillars, there is almost no difference between the pillar strength profiles predicted by the linear and power-law equations. Owing to the variability in underground rock mass and stress conditions, this debate can probably only be resolved using artificial material experiments in the laboratory under very carefully controlled testing conditions. This approach, however, also now seems problematic, as discussed further below.

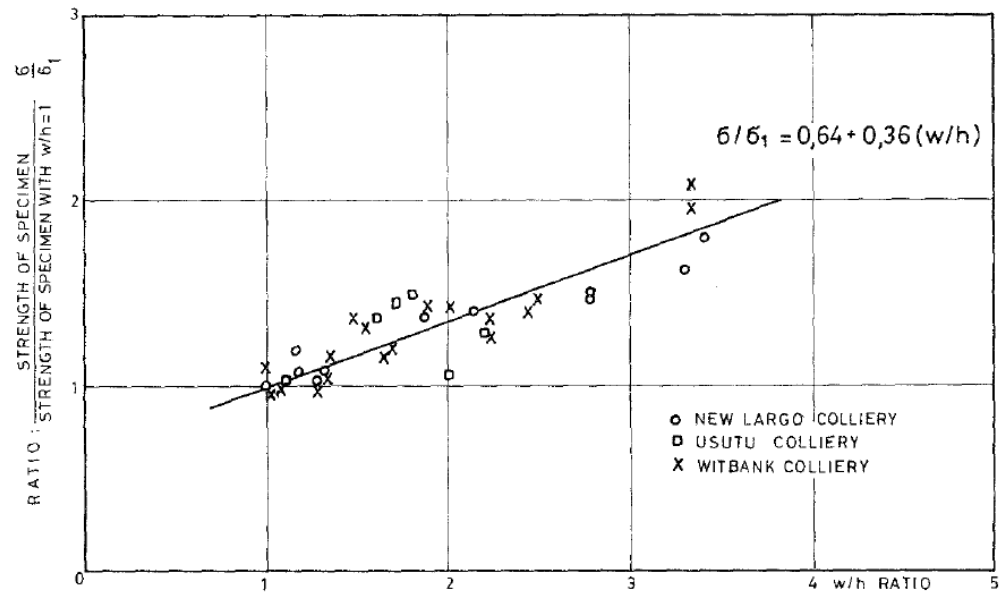

Figure 37. Pillar strength data and a fitted linear equation based on large scale in-situ tests (after Bieniawski, 1977).

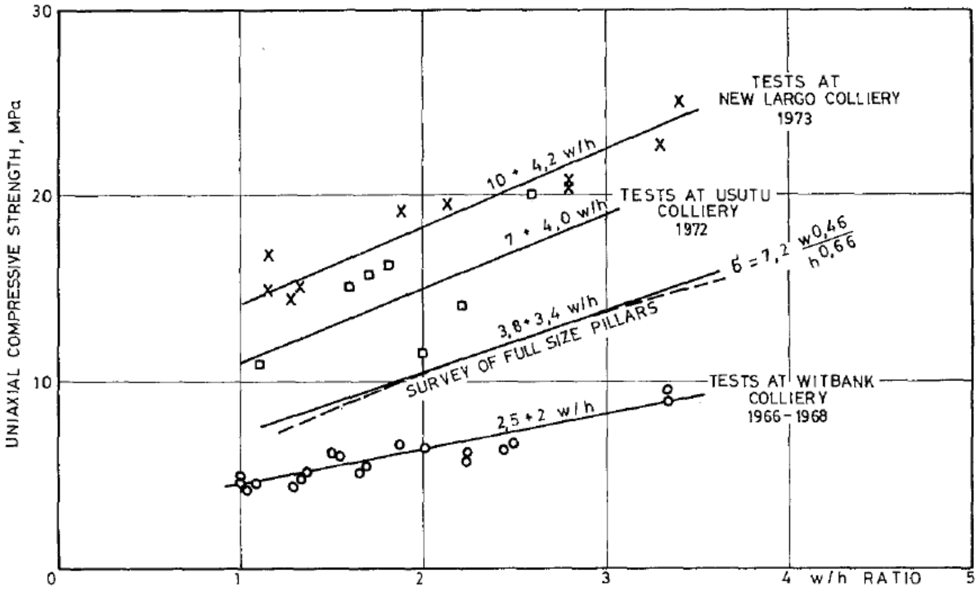

Figure 38. Comparison of coal pillar strength data from large scale in-situ tests with the two pillar formulae derived from a survey of South African coal pillars (after Bieniawski, 1977).

Of significance regarding planned future research work is that variability will also be recorded when conducting underground strength testing. Figure 39 illustrates the data used by Cook et al. (1971) in an attempt to verify the Salamon power-law strength formula. Striking is the wide scatter of the data and essentially any pillar strength formula can be fitted to this data. It is reasonable to assume that a similar variability will be found for the in-situ testing of hard rock pillars. This is concerning, as a single underground hard rock pillar mining experiment (such as that described in Napier and Malan, 2021) cannot be used to verify the applicability of any particular formula. The benefits of these large-scale underground experiments must therefore be carefully weighed against the benefits.

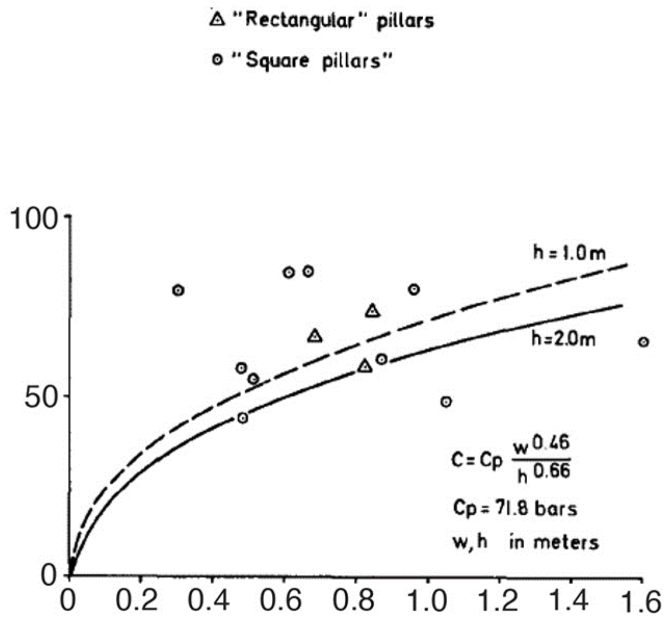

Figure 39. Experimental work to test the in-situ strength of coal pillars (after Cook et al. 1971). Note the large variability of the strength data.

This ubiquitous variability was also recently observed for laboratory experiments conducted on pillars cast from artificial material (Els and Malan, 2023). Some of these results are shown in Figure 40. Tests from the same batch of material resulted in this variability. This may even be worse when actual rock specimens are used. This casts doubt on the benefit of laboratory testing to determine the most appropriate form for a pillar formula. The variability in the strength of this artificial material will have to be minimised before samples with different width-to-height ratios can be tested.

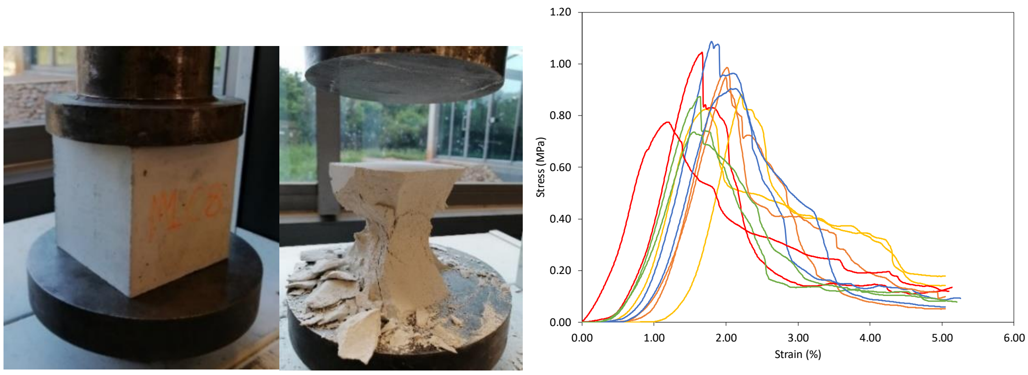

Figure 40. Laboratory testing of pillars made from an artificial material (after Els and Malan, 2023). The variability of the test results is shown on the right.

5.2 Future Research

The information presented above implies that a different approach will possibly be more successful in the future. Although an old cliché and possibly out of place in a formal report, the following quote by Einstein may be applicable: "*Insanity is doing the same thing over and over again and expecting a different result*".

Based on these considerations, a different approach is proposed as recommendations in Section 7. Four unknown aspects, playing a key role in pillar stability, are also discussed in Sections 5.2.1 to 5.2.4 below to highlight additional gaps in knowledge. These need to be explored in future research projects.

5.2.1 The effect of loading stiffness on pillar stability

Van der Merwe and Madden (2010) highlight the importance of loading system stiffness in coal mines. This has mostly been ignored in all previous studies of the stability of hard rock pillars in South Africa. Where pillar failure is possible, as in partial high extraction methods, the mode of failure is important. At Coalbrook, the pillar failure was violent, and approximately 4 000 pillars failed in a few minutes. In contrast, Van der Merwe (1999) describes a case at the Welgedacht Colliery where the pillar failure was gradual. This difference is controlled by the stiffness of the pillars and the loading system. Figure 41 highlights the two possible scenarios. For the same post peak stiffness of the pillar, the stiff overburden results in stable failure while the soft overburden results in violent failure. This concept should be explored in more detail for hard rock mines. Hard rock pillar extraction is becoming more important to extend the life of the older operations and the risk of violent collapse should be studied. Van der Merwe and Madden (2010) note that the system stiffness is reduced by a discontinuous overburden. Faults and dykes therefore reduce the stiffness of the system and increase the probability of violent failure. This possibly occurred during the infamous "hospital" collapse at Bafokeng North Mine, where the area of the collapse was bound by major geological structures running to the surface (Figure 42).

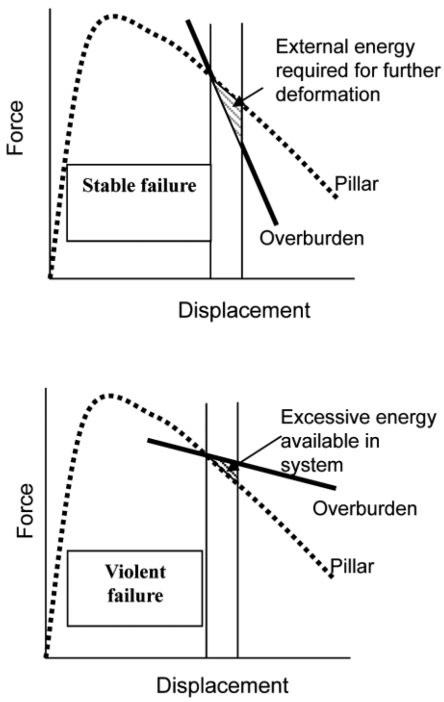

Figure 41. The concept of local system stiffness (after Salamon and Oravecz, 1976).

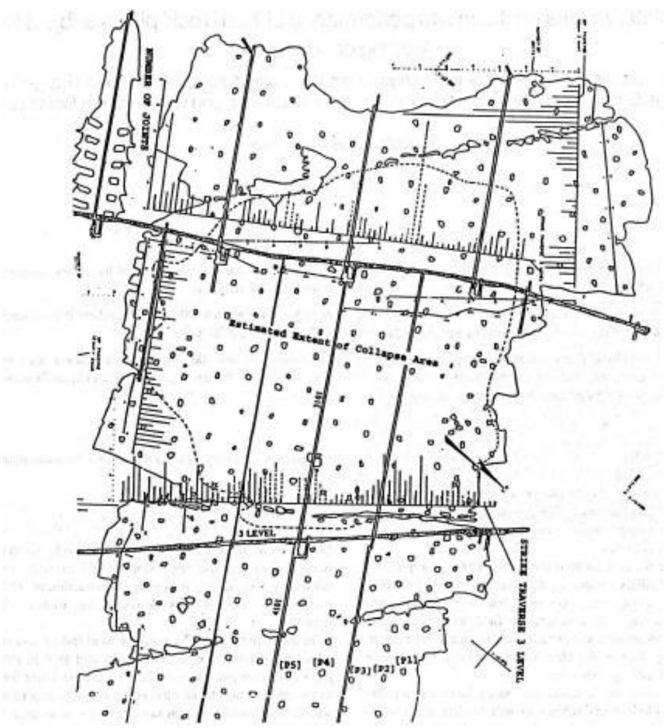

Figure 42. The extent of the collapse (dotted line) at No 6 Shaft, Bafokeng North Mine. The collapse was bound by major geological structures at the top and bottom of the figure (after Malan and Napier, 2011).

Goa et al. (2019) explored the stiffness concept and they conducted numerical modelling to calculate the local mine stiffness (LMS). This is easily calculated when mining out a pillar using the following formula (see Figure 43 for a definition of the terms):

$$K_{LMS} = \frac{f_1}{d_2 - d_1} \tag{26}$$

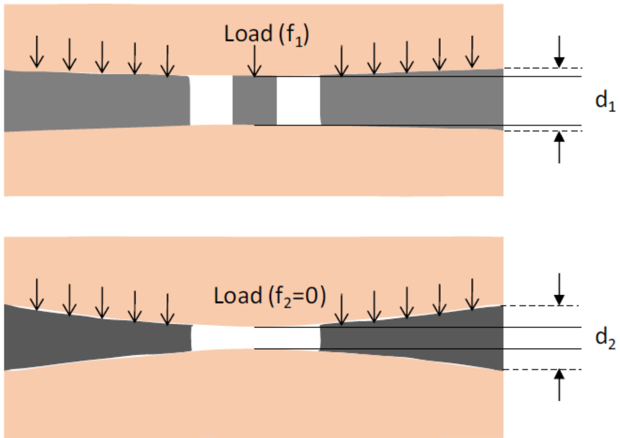

Figure 43. Local mine stiffness calculation using numerical modelling (after Goa et al, 2019).

5.2.2 Variability in pillar strength and geostatistical pillar strength determination

An aspect mostly ignored to date is that the pillar strength may vary in the different production sections of a particular mine. Typically, only one pillar design is presented by the rock engineer and this is used for all areas in the mine. A classic example is in the manganese mines, where the pillar strength is dependent on the density of the joints in the pillars (Figure 44). Only a single calibrated pillar strength formula is used in the mines, however. This may result in too low an extraction ratio for the areas with strong pillars and too high an extraction ratio for the areas with weaker pillars. Recognising this variability may be valuable to optimise the extraction ratios and improve pillar stability.

Figure 44. Different manganese pillar behaviour, in the same mine, caused by the number of joint sets and the spacing of the joints (after Wessels and Malan, 2023).

A completely unexplored aspect is the use of geostatistical methods to determine the distribution of pillar strength across the mine property. Even simple methods, such as inverse distance estimation to determine K-values for the pillar strength formula in new mining areas, may be beneficial to optimize pillar sizes. It needs to be determined, however, if this aspect is also encountered in bord and pillar mines of the other commodity types or if it is mostly confined to manganese mines.

5.2.3 Pillar reclamation in hard rock mining

Currently, a topical area that requires research is the reclamation of pillars in hard rock mines. Some of the mature mines need to implement this method to extend the life of mine. Guidelines on when this secondary mining is possible in South African mines need to be developed. The examples given below are all related to hard rock mining. An extensive description of the reclamation of coal pillars is given in Van der Merwe and Madden (2010) and it is not discussed in this report.

Haycocks (1992) indicated that partial reclamation was used in the Old Lead Belt of Missouri to increase the extraction ratio from 85% to 95%. This was normally performed towards the end of the life of the mine and partial reclamation may be the only option available when total pillar removal is not possible. He notes that pillar removal generally requires very good ground conditions. For small stoping widths, the caving that follows will “bulk” and provide some support to the roof. At greater mining heights, the hanging wall must be self-supporting or backfill must be placed.

Hustrulib and Bullock (2001) gave a brief overview of pillar reclamation. They emphasised that the most important thing to do is to install a network of convergence stations in the area in question. The convergence during reclamation must be considered in relation to typical values at the particular mine to ensure safe extraction. He listed three methods of pillar mining:

- Slabbing some ore from each pillar containing the high-grade portion of the pillar.
- Completely mining a few of the most valuable pillars, leaving enough pillars to support the area.

- Reclaiming all the pillars in a retreat sequence.

Gertsch and Bullock (1998) discuss pillar recovery and presented some case studies. They emphasise the need for rock engineering instrumentation before and during the pillar extraction process. The major variations in pillar reclamation that need to be determined are whether partial or full extraction should be attempted.

In South Africa, reclamation of hard rock pillars in bord and pillar layouts is not a common practice. One example was the “T-cutting” of some pillars at Frank I Shaft (Oosthuizen, 2005). After the initial development of the pillars, a T-shape is mined into the pillar using special trackless equipment (Figure 45). Pre-stressed elongates are installed on the shoulder as support.

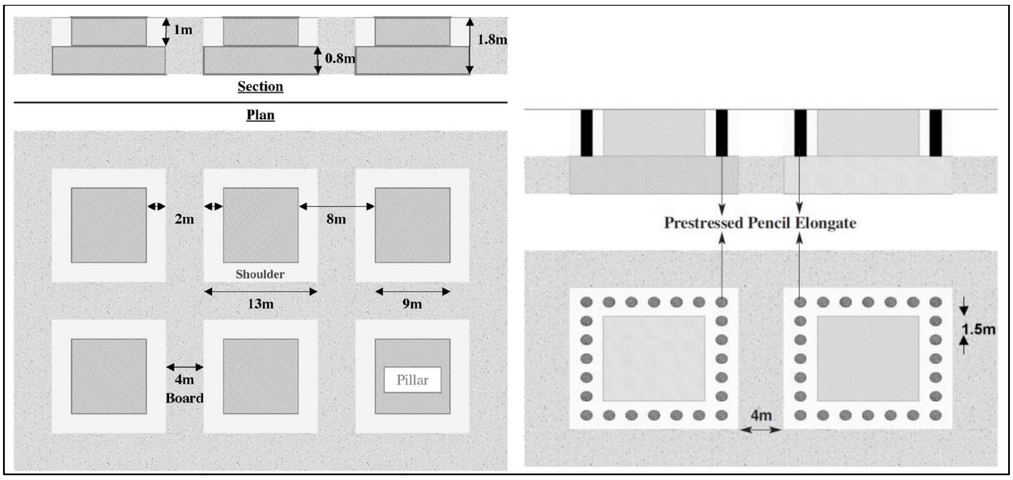

Figure 45. T-cut pillar layout at Frank I Shaft (after Oosthuizen, 2005).

The Cooke Shafts in South Africa have successfully extracted pillars for many years. This included both crush pillars used in conventional stopes and stable pillars in the mechanised bord and pillar sections. Unfortunately, this work was never published. At Cooke 3 Shaft, a grout plant was not available and so-called “Castle Packs” were used during the pillar mining. Figure 46 illustrates the installed packs.

Figure 46. Castle packs in the area where the pillars were extracted.

Numerical modelling of the area was conducted by the author using the TEXAN code and Figure 47 illustrates the proposed layout. The simulated APS before and after pillar extraction are illustrated in the figure. Note the substantial increase in APS. From the modelling, it was clear that the area extracted had to be restricted in size to prevent large scale instabilities.

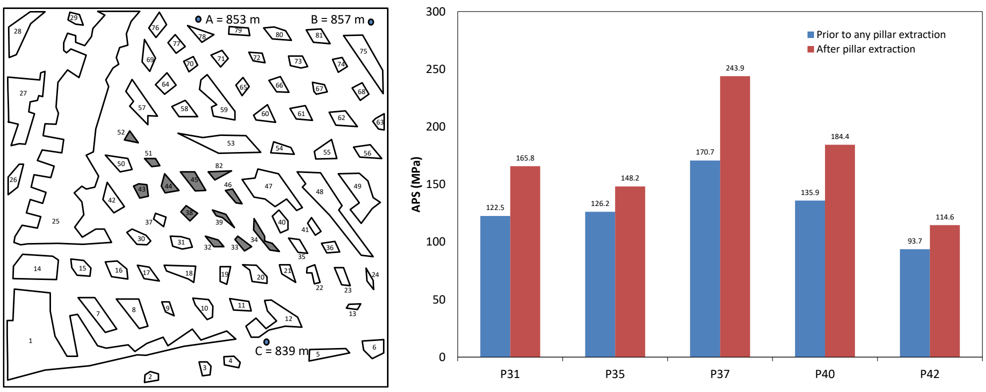

Figure 47. Numerical modelling of pillar mining. The dark coloured pillars were extracted. The stope was at a depth of approximately 850 m. The modelling results on the right illustrates the increase in APS on the surrounding pillars.

The other gold mining operation that has been successful with large scale pillar extraction is Modder East. Pillar mining started in 2017 and more than 72 000 m^2 have already been mined from pillars. The technique involves the installation of grout packs, as shown in Figure 48.

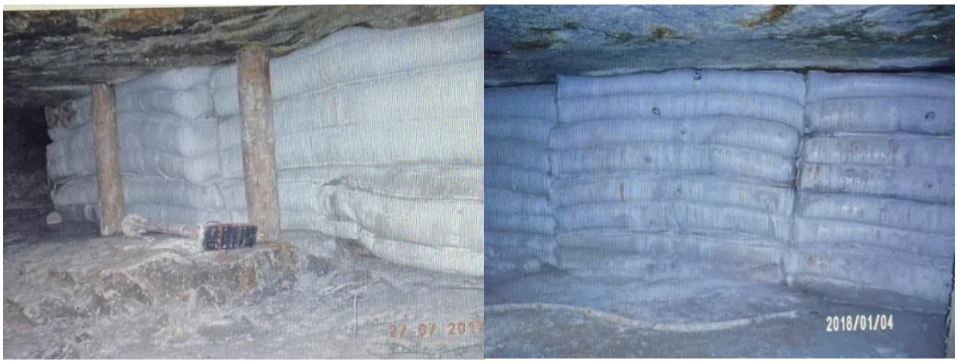

Figure 48. Grout packs used at Modder East for pillar extraction.

An important case study is the partial extraction of pillars in a chrome mine in the Rustenburg area. The orebody mined was the LG6/LG6a chromitite. The mine originally implemented a bord and pillar layout using 10 m x 14 m wide pillars. Numerical modelling was conducted to investigate the possibility of splitting the pillars in the older areas. This is illustrated in Figure 49, where the pillars are split along the long axis using a 4 m wide holing. The modelling indicated an increase in the APS of the remaining pillars, but the factor of safety was still within limits. Based on the modelling study, the mine implemented the method of splitting the pillars. The direction of splitting was later changed by the rock engineer to be in the direction of the short axis (splitting the 14 m wide side). According to the rock engineer, this worked very well and no problems were experienced during the pillar mining process. The slots through the pillars were supported using bolts.

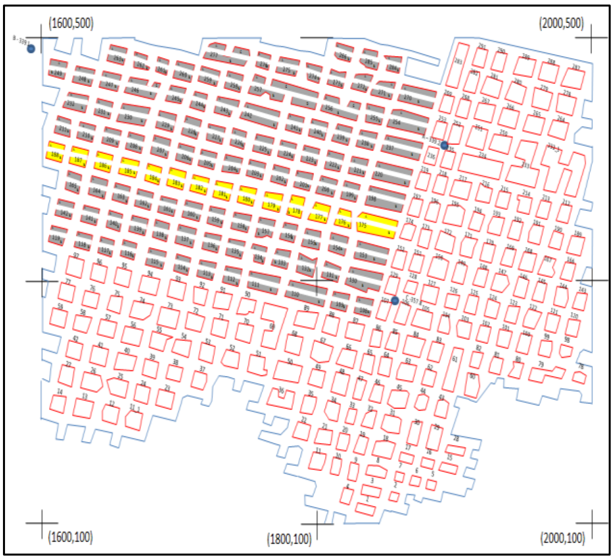

Figure 49. Layout of the chrome mine in the Rustenburg area where pillar mining was implemented. The grey pillars were some of the larger pillars and in this numerical model they were split in two using a 4 m wide holing.

Pillar reclamation can make a meaningful contribution to extending the lives of older bord and pillar mines and the feasibility for different reef types and geotechnical conditions needs to be explored in a research study. It is currently not known if a partial reclamation should be considered compared to a full extraction of all pillars, with the resulting caving in the reclamation areas. It is not clear if the collapses can be induced in a controlled fashion. In terms of coal mining, Van der Merwe and Madden (2010) describe the risk as follows:

"*Where strong layers exist in the immediate roof, the collapse of the goaf can be traumatic. In the absence of a strong layer, the roof breaks up in small portions and the collapse process is a gradual one. However, when it hangs up for long distances, it tends to fail in a single mass. It then acts as a piston, displacing air at sufficiently high velocities to result in damage to ventilation stoppings and conveyor belts and possible injury to people*."

This aspect needs to be explored in more detail for hard rock pillar reclamation. Understanding the system stiffness and how this change during pillar extraction is a key component of this work. This aspect is therefore closely linked to Section 5.2.1.

5.2.4 Effect of shear stress on pillar strength

Pillars in orebodies with a significant dip can lead to significant shear stresses in pillars. In terms of strength, Das et al (2019) noted: "*The strength of an inclined coal pillar should be estimated by considering the inclination of the coal seam and its associated behaviour, because the shearing effect along the true dip aggravates the instability of the inclined coal pillars.*" Furthermore, a back analysis of the pillar collapses experienced at Troy Mine in Montana revealed that the pillars were subject to shear stresses that lowered their capacity, as shear stresses result in a significant loss of confinement in the pillar core (Garz-Cruz et al. 2019). Shear stresses resulted in a significant loss of confinement in pillar cores (many theoretically in tension), even at width-to-height ratios that would be deemed stable under zero shear stress (flat seam under flat topography). The use of design methods that do not consider the detrimental effect of shear stress on pillar capacity may result in under-designed pillars.

The standard pillar design methodology in South Africa uses the APS as an input parameter. This is obtained from the stress acting normal to the plane of the excavation. For horizontal reefs, no shear stress acts on the pillars. This is not the case of dipping reefs and the effect of the shear stress should be quantified. Figure 50 illustrates the more complex stress components for a limit equilibrium model if the reef is inclined.

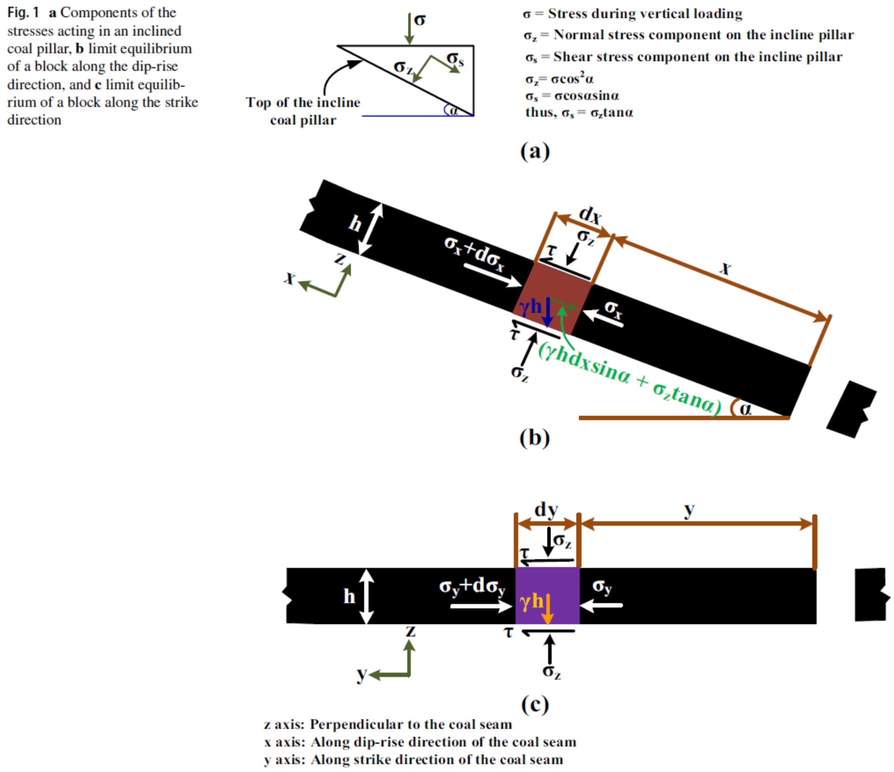

Figure 50. Stress components of a limit equilibrium model for a dipping reef (after Das et al. 2019).

6 CONCLUSIONS

The objective of this study was to determine the most appropriate type of pillar strength formula to use when designing bord and pillar layouts. As part of this project, a careful study of historical motivations for the different types of pillar strength formulae was conducted. The power-law strength formulae, made famous by Salamon and Munro (1967), were inspired by laboratory and underground experiments in the 1940s and 1950s. These indicated that the strengths, or "resistance to crush", of square pillars of the same height vary as the square root of their widths. The strengths of pillars of the same width also vary in inverse ratio to their height. This was generalised by Salamon in a power-law formula with the familiar exponents with α and β. These exponents were calibrated using a database of failed and intact pillars. For the hard rock strength formula, Hedley and Grant (1972) used the same coal work in the 1940s and 1950s, as well as Salamon's paper to motivate the use of a power-law equation. Bieniawski (1968) also did extensive underground experiments on different size coal specimens. An important finding of his investigation was that there appeared to be no change in strength once the specimen size of 1.5 m was reached. Based on this work, he proposed the simpler linear pillar strength formula. Martin and Maybee (2000) list the hard rock pillar formulae that were developed in later years based on observed pillar failures. Of significance is that these take the form of either a power- or linear-type equation and that both of these equations have been used to predict the pillar strength for a wide range of pillar shapes and rock mass strengths. No conclusive evidence could be found in this study that indicate which type of formula is more applicable. It is clear that laboratory experiments on different sizes cubes of Merensky Reef, UG2 and other chromitites will have to be done to determine if the pillar strength is better approximated by a linear or a power-law formulation. As a cautionary note, however, these experiments are notoriously difficult to do and the variability in strength results may not provide a clear answer.

The report describes a literature study of the effect of cube specimen size on the compressive strength of rock in the laboratory. All the studies reviewed indicated that laboratory rock strength decreases with increasing specimen size. This behaviour can be best described with a power-law, which includes the cube length as the controlling parameter. The exponent of this law has the typical value of ≈ -½. The drawback of this model is that it predicts that the pillar strength will eventually completely vanish for very large cube sizes. This is considered unreasonable and the model is probably only relevant to laboratory-sized specimens. Bieniawski (1968) attempted to circumvent this problem by describing the strength after a critical size with a linear strength function. Some limited laboratory data of cube specimen testing for Merensky Reef is available, but further laboratory testing on Merensky Reef, UG2 and other chrome reefs is recommended to verify that a similar power-law applies to all the hard rock reefs studied in this project. Laboratory testing of rectangular prisms, with similar square bases but different heights, needs to be conducted to supplement the testing of cube specimens.

This report is a summary of the gaps in knowledge regarding pillar strength identified in the previous milestones and pillar projects. A key aspect of this study was to test the hypothesis of whether a linear formula is better suited to describe the pillar strength in the South African mines compared to a power-law formula. It was found that there is still uncertainty in this regard and both the power-law and linear formulae, and variations of these, are used widely. It appears that the problem of finding a "universal" strength equation is caused by the variability in the measured strength of pillars, both in the laboratory and in actual mines. It is difficult to fit strength equations to the results because of the wide scatter of the data. Based on these considerations, a different approach in terms of future research is proposed. To make a further meaningful contribution in a short period of time, it is proposed that future work focus on two aspects. These are back analyses of carefully selected bord and pillar layouts to estimate the pillar strength and numerical modelling of the stiffness of the loading system. This is described in more detail below.

7 RECOMMENDATIONS

The difficulty with many of the unknowns listed above is that it will require significant resources and complex underground experimental work that will be difficult to execute. Carefully designed and expensive pillar experiments may possibly also not yield the outcomes desired as described above. Improved pillar strength formulae are nevertheless urgently required. To make a meaningful contribution to pillar research, it is proposed that future work initially focusses on two aspects and these are described below. Especially the work in Section 7.1 may result in practical outcomes that mines can implement in the shortest period of time.

7.1 Back analysis of bord and pillar layouts to estimate pillar strength

Some of the most useful pillar work in which the authors have been involved with, has been the back analysis of pillar layouts. This work, over a period of approximately fifteen years, was done mostly as consultancy projects for various mining groups or as part of larger research projects. An example is the 2021 Samerdi report: MMS21WP3 - Milestone 3 & 4 – Numerical simulation of pillar stability at the Styldrift Mine. The Merensky pillars at the mine have been substantially reduced in size and this resulted in significant spalling of the pillars. A back analysis of the layouts indicated a K-value of 90 MPa for the power-law strength formula. This supported an earlier back analysis of Merensky pillars at Impala 14 Shaft in 2011 where a similar value was obtained. This Merensky Reef K-value is deemed more accurate than approaches where, for example, a third of the UCS of the laboratory testing is used as a value. It will be of significant benefit if additional back-analysis studies can be conducted in carefully selected areas. With the necessary permissions, the old consultancy material can also be assembled to update the existing strength formulae.

The proposed project is therefore:

- Assemble all the historic back-analysis studies done on pillar strength. This may involve studies done by the various rock engineering consultancy firms. Permission will have to be obtained from the various mining groups to use the data.
- Identify key areas in the industry for further back analysis. These areas need to be selected with extreme care. This will typically be areas where pillar extraction is done or extensive pillar spalling is observed. It is expected that the factors of safety on these pillars will be much lower than in normal mining areas and better estimates of the maximum pillar strength can be obtained.
- Sites should ideally be selected for the Merensky Reef, UG2, MG chromitite and LG6 chromitite.
- Compile a database of back calculated pillar strength and the most appropriate calibration of the pillar strength formulae. This can be done for both the power-law and linear formulae.

This project will therefore still implicitly assume that these two formulae are reasonable approximations of pillar strength. Other aspects, such as the dip of the reef and shear stress, will also be considered when it is part of a particular site analysed.

7.2 Numerical modelling of stiffness of the loading system

It is proposed to use the TEXAN code to do simulations of pillar extraction and to calculate the local system stiffness. Practical aspects studied will include the changes in the system stiffness as pillar reclamation, in different sequences, is implemented.

The proposed project is therefore:

- Conduct a literature study on the use of stiffness calculations in pillar layouts using numerical codes.

- Explore the use of stiffness calculations in TEXAN and the ability of the code to simulate this behaviour
- Conduct numerical modelling experiments on different pillar extraction methodologies and the value of the stiffness calculations. The limit equilibrium model in TEXAN will be used in these simulations to simulate the pillar failure of the remaining pillars.

8 REFERENCES

Bieniawski, Z.T. 1968a. The effect of specimen size on compressive strength of coal, Int J Rock Mech Min Sci & Geomech Abstr, 5(4):325-335.

Bieniawski, Z.T. 1968b. The compressive strength of hard rock. Tydskrif vir Natuurwetenskappe, 8(3-4).

Bieniawski, Z.T. and Van Heerden, W.L. 1975. The significance of in situ tests on large rock specimens. Int. J. Rock Mech. Min. Sci. & Geom. Abstr. 12.

Bieniawski, Z.T. 1977. Discussion - A Review of Coal Pillar Strength Formulas by W. A. Hustrulid, Rock Mechanics, 10 pp. 107-110.

Bieniawski, Z.T. 1992. A method revisited: coal pillar strength formula based on field investigations. Proc. Workshop on coal pillar mechanics and design. US Bureau of Mines IC 9315.

Celik, S.B. 2017. The effect of cubic specimen size on uniaxial compressive strength of carbonate rocks from Western Turkey, Arab J Geosci, 10: 426.

Cook, N. G. W., Hodgson, K. and Hojem J. P. M., 1971. A 100-MN jacking system for testing coal pillars underground. J. S. Afr. Inst. Min. Metall., June 1971. pp. 215-224.

Couto, P.M. and Malan, D.F. 2023. A Limit Equilibrium Model to Simulate the Large-Scale Pillar Collapse at the Everest Platinum Mine. Rock Mech Rock Eng 56, 183–197.

Das, A.J., Mandal, P.K., Paul, P.S. and Sinha, R.K. 2019. Generalised analytical models for the strength of the inclined as well as the flat coal pillars using rock mass failure criterion. Rock Mechanics and Rock Engineering 52:3921–3946.

Els, R.P. and Malan, D.F. 2023. Calibration of the limit equilibrium pillar failure model using physical models. Submitted to J. S. Afr. Inst. Min. Metall.

Esterhuizen, G.S. 2014. Extending empirical evidence through numerical modelling in rock engineering design, Journal of the Southern African Institute of Mining and Metallurgy, 114:755-764.

Esterhuizen, G.S., Dolinar, D.R., and Ellenberger, J.L. 2008. Pillar Strength and Design Methodology for Stone Mines. Proceedings of the 27th International Conference on Ground Control in Mining, West Virginia University, Morgantown WV, 2008, pp 241–253.

Gao, F., Kang, H., Lou, J., Li, J. and Wang, X. 2019. Evolution of Local Mine Stiffness with Mining Process: Insight from Physical and Numerical Modeling, Rock Mechanics and Rock Engineering 52:3947–3958.

Garza-Cruz, T., Pierce, M. and Board, M. 2019. Effect of Shear Stresses on Pillar Stability: A Back Analysis of the Troy Mine Experience to Predict Pillar Performance at Montanore Mine. Rock Mech Rock Eng 52, 4979–4996.

Gertsch, R.E. and Bullock R.L. 1998. Techniques in underground mining: selections from Underground mining methods handbook, SME

Greenwald, H.P., Howarth, H.C. and Hartmann, I. 1939. Experiments on the strength of small pillars of coal in the Pittsburgh bed. U.S. Bur., Min., Tech. Pap. 605.

Greenwald, H.P., Howarth, H.C. and Hartmann, I. 1941. Progress Report - Experiments on the strength of small pillars of coal in the Pittsburgh bed. U.S. Bur., Min., June 1941.

Haycocks, C. 1992. Stope and pillar mining, Chapter 18.2. In: Hartman, H.L. (ed) SME mining engineering handbook, Volume 2, Society for Mining, Metallurgy and Exploration Inc.

Hedley, D.G.F. and Grant, F. 1972. Stope-and-pillar design for the Elliot Lake Uranium Mines. Bull Can Inst Min Metall 65:37-44.

Hedley, D.G.F. and Roxburgh, J.W. and Muppalaneni, S.N. 1984. A case history of rockbursts at Elliot Lake. In: Proceedings of 2nd International Conference on Stability in Underground Mining, Lexington. New York: American Institute of Mining, Metallurgical and Petroleum Engineers, Inc., p. 210234.

Heuze, F.E. 1980. Scale effects in the determination of rock mass strength and deformability. Rock Mech 12:167–192.

Holland, C.J. and Gaddy, F.L. 1957. Some aspects of permanent support of overburden on coal beds. Proc. West Virginia Coat Min. Inst.

Hudson, J.A., Brown, E.T. and Fairhurst, C. 1972. Shape of the complete stress-strain curve for rock. In: Cording E, editor. Proceedings of 13th US Symposium on Rock Mechanics, Urbana. New York: American Society of Civil Engineers, p. 773-795.

Hustrulid, W.A. 1976. A review of coal pillar strength formulas. Rock Mechanics, 8:115-145.

Hustrulib, W.A. and Bullock, R.L. 2001. Underground Mining Methods: Engineering Fundamentals and International Case studies, SME.

Kersten, R.W.O. 1984. The design of pillars in the shrinkage stoping of a South African gold mine. J.S. Afr. Inst. Min. Metall., 84(11):365-368.

Krauland N, Soder PE. 1987. Determining pillar strength from pillar failure observations. Eng Min J. 8:34-40.

Lunder, P.J. and Pakalnis, R. 1997. Determining the strength of hard rock mine pillars. Bulletin of the Canadian Institute of Mining and Metallurgy. 90:51–55.

Malan, D.F. and Napier, J.A.L. 2011. The design of stable pillars in the Bushveld mines: a problem solved? J S Afr Inst Min Metall 111:821–836.

Malan, D.F. and Napier, J.A.L. 2021. A review of the role of underground measurements in the historic development of rock engineering in South Africa, J. S. Afr. Inst. Min. Metall, 121(5):201–216.

Madden, B.J. 1991. A re-assessment of coal pillar design. Journal of the South African Institute of Mining and Metallurgy. 91:27-37.

Martin, C.D. and Maybee, W.G. 2000. The strength of hard-rock pillars. Int. J. Rock. Mech. Min. Sci. 37:1239-1246.

Napier, J.A.L. 2018. Progress report on face edge failure and mining rate simulation. Unpublished research report, University of Pretoria.

Napier, J.A.L. and Malan D.F. 2021. A limit equilibrium model of tabular mine pillar failure. Rock Mechanics and Rock Engineering, 54:71-89.

Oosthuizen, C.C. 2005. Bord and pillar applications on the platinum mine: T-cut mining method, J. S.Afr. Inst. Min. Metall., vol. 105, pp. 187- 191.

Ozbay, M.U., Ryder, J.A. and Jager, A.J. 1995. The design of pillar systems as practiced in shallow hard-rock tabular mines in South Africa, J S Afr Inst Min Metall, pp. 7 – 18.

Potvin, Y., Hudyma, M.R. and Miller, H.D.S. 1989. Design guidelines for open stope support. Bull Can Min Metall 82:53-62.

Pratt, H.R., Black, A.D., Brown, W.S. and Brace, W.F. 1972. The effect of specimen size on the mechanical properties of unjointed diorite. Int. J. Rock Mech. Min. Sci. & Geomech. Abstracts 9:513–529.

Roberts, D., Tolfree, D. and Mcintyre, H. 2007. Using confinement as a means to estimate pillar strength in a room and pillar mine. Proceedings of the 1st Canada-US Rock Mechanics Symposium. Taylor and Francis. 1455–1461.

Ryder, J.A. and Jager, A.J. 2002. A textbook on rock mechanics for tabular hard rock mines, SIMRAC, Johannesburg.

Salamon, M.D.G. and Munro, A.H. 1967. A study of the strength of coal pillars. J. S. Afr. Inst. Min. Metall. 68:55–67.

Salamon, M.D.G. and Oravecz, K.I. 1976. Rock Mechanics in Coal Mining. Chamber of Mines of South Africa. P. R. D. Series No. 198.

Sjoberg, J. 1992. Failure modes and pillar behaviour in the Zinkgruvan mine. In: Tillerson JA, Wawersik WR, editors. Proceedings of 33rd U.S. Rock Mechanics Symposium, Sante Fe. Rotterdam: A.A. Balkema, pp. 491-500.

Skinner, W.J. 1959. Experiments on the compressive strength of anhydrite. The Engineer, February 1959.

Steart, F.A. 1954. Strength and stability of pillars in coal mines.' J. Chem. Metall. Min. Soc. SA Vol. 54, pp. 309-325.

Van der Merwe, J.N. 1999. New strength formula for coal pillars in South Africa. Proc. 2nd Intnl Workshop on Coal Pillar Mechanics and Design, Vail, CO, USA.

Van der Merwe, J.N. and Madden, B.J. 2010. Rock engineering for underground coal mining, SAIMM Special Publications Series 8.

Von Kimmelmann, M.R., Hyde, B. and Madgwick, R.J. 1984. The use of computer applications at BCL Limited in planning pillar extraction and design of mining layouts. In: Brown ET, Hudson JA, editors. Proceedings of ISRM Symposium: Design and Performance of Underground Excavations. London: British Geotechnical Society, pp. 53-63.

Wagner, H. and Salamon, M.D.G. 1979. Pillar design. Series of Lectures given at Sappers Rust, Pretoria, Aug. 1979.

Watson, B.P., Ryder, J.A., Kataka, M.O., Kuijpers, J.S. and Leteane, F.P. 2008. Merensky pillar strength formulae based on back analysis of pillar failures at Impala Platinum, J. S. Afr. Inst. Min. Metall., 108:449 – 461.

Wessels, D.G. and Malan, D.F. 2023. A limit equilibrium model to simulate time-dependent pillar scaling in hard rock bord and pillar mines. Rock Mechanics and Rock Engineering.

York, G. and Canbulat, I. 1998. The scale effect, critical rock mass strength and pillar system design, J.S. Afr. Inst. Min. Metall., 98.